

5

ACCOUNTING FOR CARBON IN ARTOCARPUS ALTILIS AFFORESTATION SYSTEMS

10 A THESIS SUBMITTED TO THE GRADUATE DIVISION OF THE UNIVERSITY OF HAWAI'I AT MĀNOA
IN PARTIAL FULFILLMENT OF THE REQUIREMENTS FOR THE DEGREE OF

MASTER OF SCIENCE

IN

TROPICAL PLANT AND SOIL SCIENCES

15

OCTOBER 2023

By

Chad M. Livingston

20

Thesis Committee:

Dr. Noa K. Lincoln, Chairperson

Dr. Jonathan Deenik

Dr. Susan Crow

25

Keywords: breadfruit, AGB, Soil Carbon, Terrestrial Carbon

ACKNOWLEDGEMENTS

30 This work was funded by a McIntire-Stennis Capacity Grant from the USDA NIFA and administered by the College of Tropical agriculture And Human Resources. From the start, I have been a non-traditional student; a special thanks to Dr. Noa Lincoln, the rest of my committee, and TPSS leadership for their patience and support as I worked through the program.

ABSTRACT

As the impacts of climate change accelerate, the need for climate-smart agriculture—crops and systems with a high degree of productivity that are both resilient to a changing environment and reduce greenhouse gas emissions—will only increase. Once a substantial source of calories in the Hawaiian Islands and elsewhere around the Pacific, *Artocarpus altilis*, or breadfruit, has been suggested as an agricultural product that meets these standards. Among its potentially climate-smart attributes, breadfruit has the potential to store carbon in its biomass, and accompanying farming practices such as co-cropping could potentially increase carbon storage within the soil. To begin to elucidate some of these attributes, this study explored the terrestrial carbon pools associated with breadfruit afforestation by 1) quantifying above-ground biomass (AGB), 2) extrapolating to landscape-scale impacts by reviewing the below-ground biomass (BGB) and creating growth curves for breadfruit, and 3) conducting a cursory exploration of dead organic matter (litter) and soil organic carbon. The study followed guidelines and methods published in the scientific literature and carbon accounting documents to develop the allometry to describe AGB and growth of *A. altilis* over time, and based on this estimate, employed a root-to-shoot ratio to estimate BGB. We employed a standard sampling technique to estimate litter mass and its associated carbon content and developed a sampling design to describe total and hot water extractable soil organic carbon present within a subsection of the breadfruit orchard. This thesis' primary contribution to the body of literature is the development of a novel allometric equation that describes AGB and carbon in terms of diameter at breast height (DBH) in *A. altilis* $AGB = -4.586 + 0.1635 \times DBH + 0.2229 \times DBH^2$. Applying these equations approximately 10 years into an afforestation project each breadfruit tree contains approximately 90.2 kg Carbon in above- and below- ground biomass. In comparison, the litter sampling effort arrived at an estimated .538 kg Carbon per tree in the surface layer of litter and the soil carbon sampling showed no significant changes in soil carbon over the same timeframe. The thesis concludes that breadfruit has a significantly higher potential to sequester carbon compared to other annual staples, with most of the sequestration occurring in the trees' biomass. In combination with existing data supporting breadfruit's ability to adapt to various climate change scenarios, we agree with the previous assessments that prioritize *A. altilis* as a climate-smart commodity.

60

TABLE OF CONTENTS

	Acknowledgements.....	ii
	Abstract.....	iii
65	List of Tables.....	vi
	List of Figures	vii
	List of Abbreviations.....	viii
	CHAPTER 1. INTRODUCTION	1
70	CHAPTER 2. DEVELOPMENT OF A. <i>ALUTILIS</i> ALLOMETRY AND CHARACTERIZATION OF ABOVE-GROUND CARBON STORAGE IN HAWAI'I	3
	2.1. Introduction.....	3
	2.2. Background on Allometric Equation Development.....	4
	2.3. Methods	7
	2.3.1. Overview.....	7
75	2.3.2. Woody Biomass Volumetric Estimation.....	7
	2.3.3. Wood Density and Carbon Content.....	8
	2.3.4. Foliar Biomass Estimation	8
	2.3.5. Statistical Analysis	8
	2.4. Results	10
80	2.4.1. Wood Density and Carbon Density	10
	2.4.2. Foliar Biomass	12
	2.4.3. Woody Biomass Volume.....	13
	2.5. Discussion	15
	3.1. Introduction.....	17
85	3.2. Background	18
	3.2.1. Describing Growth of DBH over time	18
	3.2.2. Belowground Biomass (BGB).....	18
	3.3. Methods	19
	3.3.1. Tree Growth Evaluation.....	19
90	3.3.2. Extrapolation of Landscape-scale Carbon Sequestration in Breadfruit Biomass Over Time.....	19
	3.4. Results	20
	3.4.1. Growth.....	20
	3.4.2. Landscape Scale Carbon Estimate.....	21
95	3.4.3. Error Estimates	21
	3.5. Discussion	22

	CHAPTER 4. SENESCENCED ORGANIC MATTER POOL	23
	4.1. Introduction.....	23
	4.2. Background	23
100	4.3. Methods	24
	4.4. Results	25
	4.4.1. Layer of Surface Litter Characteristics.....	25
	4.4.2. Litter Mass and Carbon Percentage	25
	4.4.3. Estimating Carbon per Tree and Hectare.....	26
105	4.5. Discussion	26
	CHAPTER 5. SOIL CARBON POOLS WITHIN A BREADFRUIT ORCHARD IN CENTRAL OAHU OXISOL POST-PLANTATION LAND USE	27
	5.1. Introduction.....	27
	5.2. Background	28
110	5.2.1. Hot Water Extractable Carbon	28
	5.2.2. Equivalent Soil Mass	28
	5.3. Methods	28
	5.3.1. Site Description	28
	5.3.2. Sampling Description and Lab Work.....	28
115	5.3.3. Equivalent Soil Mass (ESM)	30
	5.4. Results	30
	5.4.1. Soil Mass	30
	5.4.2. Hot Water Extractable Carbon	30
	5.4.3. Organic Carbon Heterogeneity	31
120	5.5 Discussion.....	31
	CHAPTER 6. CONCLUSION	33
	6.1. Overview	33
	6.2. The Way Ahead: A Carbon Project.....	33
	6.2.1. Carbon Accounting	33
125	6.2.2. Calories per acre	34
	7. REFERENCES	35

LIST OF TABLES

130 **Table 1.** Five previously published allometric equations. 5
Table 2. Reported wood density values of *Artocarpus* spp. 5
Table 3. Woody, foliar, and total above-ground biomass for 12 breadfruit trees 14
Table 4. Root-to-Shoot ratios..... 19
Table 5. Equations describing the growth in DBH 21
135 **Table 6.** Extrapolation of diameter at breast height (DBH) to total carbon (Total C)..... 21
Table 7. Root Mean Square Error of Associated Models 22
Table 8. Litter characteristics of *Artocarpus* spp. from published studies. 24
Table 9. Litter characteristics..... 26
Table 10. Results from the HWEC 30
140 **Table 11.** Results from hot water extractable and total soil carbon 31

145

150

155

160 LIST OF FIGURES

Figure 1. Schematic diagram compartmentalizing tree measurements..... 6
Figure 2. Conceptual diagram illustrating spreadsheet model to calculate total biomass 9
Figure 3. Linear regression of the dry wood density against radius..... 10
Figure 4. Linear regression of percent carbon as a function of stem radius 11
165 **Figure 5.** Linear regression of carbon density (gC/cm³) as a function of stem radius 12
Figure 6. Foliar biomass as a function of terminal branch stem radius 13
Figure 7. Quadratic regression of total AGB against DBH 14
Figure 8. Graphical comparison of allometric equations 15
Figure 9. Illustration of the litter sampling methodology 25
170 **Figure 10.** Illustration of soil sampling experimental design 30

LIST OF ABBREVIATIONS

AGB: Above Ground Biomass

BGB: Below Ground Biomass

DBH: Diameter at Breast Height

175 FAO: Food and Agricultural Organization of the United Nations

GHG: Greenhouse Gas

HWEC: Hot Water Extractable Carbon

IPCC: International Panel on Climate Change

180

CHAPTER 1. INTRODUCTION

Globally, agricultural activities and associated deforestation account for an estimated 24% of anthropogenic greenhouse gas (GHG) emissions, and demand for land to support globalized food industry supply chains is a major driver of deforestation (Garnett 2013; Rockstrom et al. 2020). A central question for humanity will increasingly focus on how to build climate-smart food systems. As defined by the Food and Agriculture Organization of the United Nations (FAO), the three pillars of climate-smart agriculture are increasing agriculture productivity and incomes, adapting and building the resilience of people and agriculture systems in the face of climate change, and reducing or even eliminating greenhouse gas emissions (FAO 2021).

This problem is not entirely dissimilar to the challenges faced by the early inhabitants of the remote Pacific Islands. As human populations on these islands grew, developing agricultural systems that provided adequate food and resources but that did not result in ecosystem collapse became matters of survival. Among the diverse agroecological strategies employed, forest management and arboriculture were critical, often dominant, forms of food and resource production that maintained the integrity and function of the ecosystem (Lincoln and Vitousek 2017; Lincoln, Haensel, and Lee 2023; Quintus et al. 2019; Winter et al. 2018). Breadfruit – a long-lived tree that produces large fruits rich in complex carbohydrates – featured prominently in these forest management strategies, with Hawaiian cultivators developing a broad range of agroforestry systems prominently featuring breadfruit (Lincoln and Lagefoged 2014; Lincoln 2020a).

Breadfruit, and breadfruit agroforestry, remain vastly understudied despite significant international recognition of the potential roles of the crop in developing climate-smart agriculture and addressing global hunger (Lucas and Ragone 2012) and demonstrated contributions to food system resilience (Berning et al. 2022). Breadfruit not only has the potential to sequester carbon in its biomass, but its cultivation often accompanies farming practices such as reduced- or no-tillage and cover- or co-cropping that can further increase carbon storage in other pools, such as soil carbon. For human nutrition, breadfruit supplies complex carbohydrates associated with a strong profile of vitamins, minerals, and amino acids (Jones et al. 2011; Needham, Jha, and Lincoln 2020; Lucas and Ragone 2012). From a social/economic perspective, tree crops need only be planted once, reducing annual farm labor and thereby enhancing farmer profits and quality of life. With proper management, breadfruit trees require little care, as weeds are largely controlled through shade and companion plantings that potentially reduce the need for pesticide usage – protecting the health of farmers and their families. Within the Pacific, breadfruit furthermore impacts biocultural restoration to support the restoration of cultural practices, knowledge, and equity (Langston and Lincoln 2018, Lincoln 2020b).

Because of its potential role in climate-smart agriculture, breadfruit is a candidate for both formal and informal carbon market projects. In 2017, Hawai'i mandated that agricultural, aquacultural, agroforestry, and forestry projects, must satisfy a carbon registry's approved carbon accounting protocols (Act 033,

SLH 2017). These protocols derive from science-based publications of governmental and non-governmental organizations such as the International Panel on Climate Change (IPCC) and Verified Carbon Standard (VCS). However, carbon accounting protocols and the development of carbon market projects remain relatively incomplete, and protocols and methodologies do not yet exist to cover all
220 situations. In particular, tropical and indigenous crops, including breadfruit, are understudied and poorly represented in existing protocols and models (Padulosi et al. 2002; Lincoln et al. 2018). Therefore, although the IPCC and not-for-profit organizations have developed the carbon project methodologies based on scientific methods, tailoring existing protocols and methodologies to a specific situation, such as breadfruit agroforestry, requires additional research.

225 This thesis applies carbon accounting methodologies to develop quantitative data on the terrestrial carbon pools of Hawaiian breadfruit orchards, with an emphasis on the above-ground biomass (AGB) pool, and a cursory exploration of the below-ground biomass (BGB) pool, the soil organic carbon pool and the dead organic matter (litter) pool. This effort importantly contributes the first breadfruit-specific allometric equation to define AGB and informs future work and discussions of a potential role for
230 breadfruit as a climate-smart crop, including the development of breadfruit-focused carbon projects.

235

240

245 **CHAPTER 2. DEVELOPMENT OF *A. ALTILIS* ALLOMETRY AND CHARACTERIZATION OF ABOVE-
GROUND CARBON STORAGE IN HAWAII**

2.1. Introduction

Growing trees and vascular plants capture carbon from the air (from where?), assimilating it into their biomass. The rates of carbon assimilation vary widely by species and are further influenced by the
250 growing conditions. Because it is most easily observed and measured, the above-ground biomass (AGB), which includes leaves, stems, branches, and bole, is often separated from the total biomass, which would also include the below-ground component (i.e., roots). The ability to quantify the AGB present in forests, agriculture and other systems is vital for effective carbon accounting (Goodman et al. 2014; Litton and Boone Kauffman 2008).

255 Forestry science has developed methods to quantify the size of the AGB pool and describe changes in this pool over time. The most widely applied method for estimating tree biomass is allometry. At its foundation, allometry describes the ontological growth of individuals. There are two general definitions of allometry (Picard et al. 2015). The more restrictive definition employs a power model to describe the proportionality between relative increases in dimensions as the individual tree grows and develops, which
260 is often employed in the field of biology, rooted in the concept of idealized physiological vasculature that underlies allometric scaling theory (West, Brown, and Enquist 1997). The less restrictive definition, and the definition used throughout this study, refers to an equation that describes the relationship between common forestry measurements and AGB (Stevens 2009). Looking at trees from a population perspective, the various dimensions of an individual tree relate statistically to each other. For example,
265 diameter-at-breast-height (DBH) and AGB follow the same general relationship regardless of the size of the tree. DBH typically explains more than 95% of the variation in tree biomass, even in highly diverse forests (Brown 1997).

The accuracy of an allometric equation depends on a number of factors, with an essential element being how diverse of a population one attempts to describe. The allometric relationships will clearly vary by
270 species, but may also shift in response to climatic and site conditions, heterogeneity of growing conditions, and management effects (e.g. pruning). At one extreme, supreme accuracy (>99%) can be achieved for species and site-specific allometry of trees grown in uniform conditions, such as monotypic forestry plantations (Daba and Soromessa 2019). At the opposite extreme, generic equations can be developed to represent broad categories of trees and sites, such as broadleaf trees in tropical forests, in
275 which average accuracy for any given individual may fall well below 80% (Chave et al. 2005).

As an underutilized and understudied crop, no allometry has been developed specifically for breadfruit. Therefore, estimates of AGB carbon are restricted to either using allometry for related species or applying generic equations describing general tree types. Only a single allometric study was identified for any member of the Artocarpus family (jackfruit, *A. Heterophyllus*; Santos Martin et al. 2010). Four relevant

280 allometric equations were identified that describe broadleaf trees in pantropical environments. However,
the five equations vary widely—over 18-fold—in their estimation of biomass. While any indirect
measurement of carbon is bound to have uncertainly, such substantial variation makes the application of
allometry to breadfruit almost useless. To complicate matters, several of these equations rely on tree
parameters such as wood and carbon density that are poorly described for the highly variable Artocarpus
285 family and which typically have no published values for breadfruit, introducing even more error and
uncertainty into the calculations.

To support the application of breadfruit as a climate-smart commodity, this study investigates the above-
ground biomass and carbon content of that biomass. Specifically, the objectives of this section are to (1)
use a non-destructive approach to characterize the volume in diameter-specific segments of *A. altilis*
290 trees in Hawai'i; (2) use minimally destructive sampling to characterize variation in wood and carbon
density as a function of branch diameter; (3) use destructive sampling to determine total leaf biomass as
a function of terminal branch diameter; (4) incorporate measurement of tree architecture, wood/carbon
density and leaf biomass into a mathematical model to determine total AGB; (5) use AGB of multiple trees
to develop an allometric equation for *A. altilis* in Hawai'i; and (6) evaluate the accuracy of previously
295 published allometric equations based on this study.

2.2. Background on Allometric Equation Development

A prominent method to develop allometric equations requires destructive sampling, in which the entire
trees are measured, dissected into components, kiln-dried, and weighed to determine the total biomass of
individuals. Destructive sampling relies on felling whole trees and submerging the component parts in
300 water to obtain volumetric estimation. Most often, the trees will be partitioned into their individual parts
(leaves, stems, branches, and boles) during this process so that general characterization of those
categories can occur. After determining volume, the mass is dried in large kiln ovens to determine the
total biomass of each tree part. Finally, average carbon density, which is not constant across plant parts
or even parts of different sizes, is determined through combustion analyses. With these calculations in
305 hand, researchers can calculate a total volume, biomass, and carbon biomass, and apply simple
statistical regressions to determine a best fit allometric equation to represent specific species or sites
(Dietze, Wolosin, and Clark 2008). This is an expensive and involved process that often results in small
sample sizes and other types of errors. Therefore, crafting accurate and valid allometric equations can be
challenging, particularly for small-scale farmers or underutilized species. A review of the literature found
310 only one allometric equation for an Artocarpus species (jackfruit, *A. Heterophyllus*) that destructively
sampled eight trees (Santos Martin et al. 2010).

Because of the difficulties involved in the destructive sampling required to develop species- or site-
specific allometry, many allometric equations rely on large data sets to build equations that apply across
classes of trees, sites, and/or conditions (Brown 1997; Chave et al. 2005) These generic equations exist

315 for practically all forests of the world (Brown 2002).^{1,2} Prime examples of generic pantropical equations include the Brown (1997) and Chave et al. (2005) models. As one would expect, the more generalized an allometric equation is, the less accurate it can be for each individual within the group. For instance, Litton and Kauffman (2008) found that these equations tended to both under and overestimate the AGB of two prominent native Hawaiian species depending on the species and DBH.

320 Several relevant allometric equations that could potentially be applied to breadfruit trees in Hawai'i were identified (Table 1), however, the identified equations vary widely in their estimation of biomass and consequently carbon. To complicate matters, there is also substantial variation in reported tree attributes that are used within these equations, such as the wood density (Table 2).

Table 1. Five previously published allometric equations to describe tree biomass (kg) that could potentially be applied to breadfruit trees in Hawai'i, including four pantropical equations built from large global datasets and one equation specific to a related *Artocarpus* species.

Description	Source	Equation
Moist, pantropical 1500–3500 mm/y precip	Brown (1997)	$ABG = e^{(-2.134 + 2.53 \times \ln(D))}$
Wet, pantropical >3500mm/y precip.	Brown (1997)	$ABG = 21.297 - (6.953 \times D) + (0.74 \times D^2)$
Moist, pantropical 1500–3500 mm/y precip.	Chave et al. (2005)	$ABG = \rho \times e^{\{-1.499 + [21.48 \times \ln(D)] + [0.207 \times (\ln(D))^2] - [0.0281 \times (\ln(D))^3]\}}$
Wet, pantropical >3500/y precip	Chave et al. (2005)	$ABG = \rho \times e^{\{-1.239 + [1.98 \times \ln(D)] + [0.207 \times (\ln(D))^2] - [0.0281 \times (\ln(D))^3]\}}$
<i>Artocarpus heterophyllus</i>	Santos Martin et al. (2010)	$ABG = 0.065 \times D^{2.28}$

D is diameter at breast height (cm) and ρ is wood specific gravity (g/cm³)

Table 2. Reported wood density values of *Artocarpus* spp. From published sources

Species (plant part)	Source	Density (g/cm ³)
<i>Artocarpus elasticus</i>	Kenzo et al. (2009)	.30
<i>Artocarpus</i> spp.	Kenzo et al. (2009)	.43
<i>Artocarpus heterophyllus</i> (avg)	Santos-Martin et al. (2010)	.45
<i>Artocarpus heterophyllus</i> (branch)	Santos-Martin et al. (2010)	.51
<i>Artocarpus heterophyllus</i> (twig)	Santos-Martin et al. (2010)	.52

325 Non-destructive approaches seek to determine the volume of the tree through detailed measurements, which can be done manually or through imaging technologies. The manual process involves measuring all woody components of a tree in compartments (Figure 1). The elliptical diameter of the bole and each primary, secondary, tertiary, and quaternary branch is recorded at each 1m increment. Beginning at the

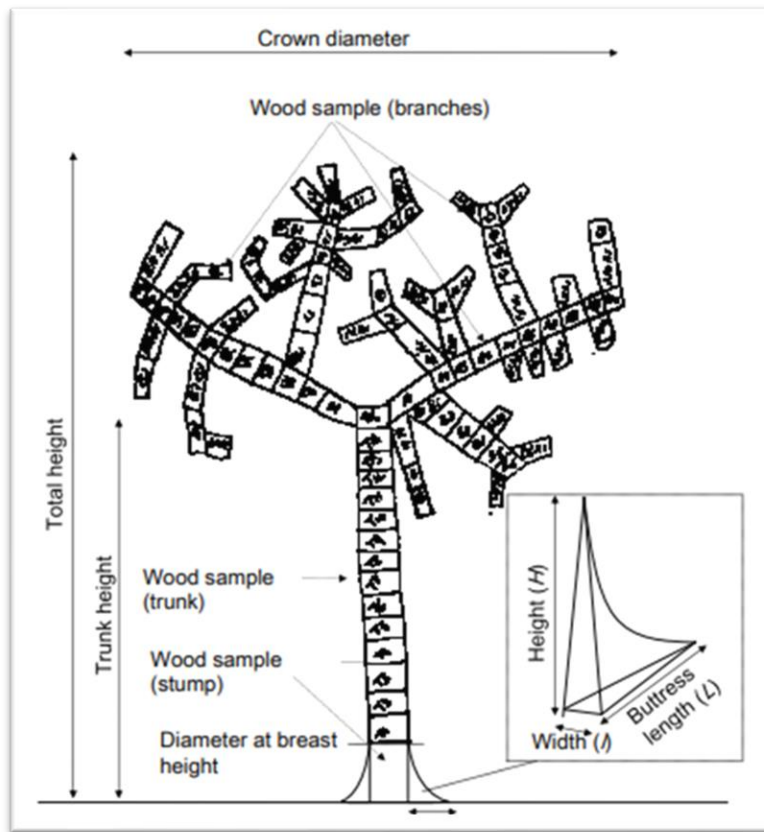
330

¹ The IPCC also aggregated significant stores of data into tables in their general guide to carbon measurement methodologies (“2019 Refinement to the 2006 IPCC Guidelines for National Greenhouse Gas Inventories” 2019.)

² Some pantropical equations include height measurements, but often the pan-tropical equations exclude height because of the often-close relationship between height and diameter (Ketterings et al. 2001) and most inventory studies employ DBH and height for commercial trees (Litton and Kauffman 2008).

1.3m DBH mark the diameter is recorded as D_1 and then following along the branch 1m later the second diameter is recorded as D_2 . The same procedure is repeated for the next 1m compartment using D_2 as the starting point for the next compartment. The volume of each compartment is then often calculated using the truncated cone taper function or a simple conic function and the total volume of the tree is calculated as the sum of the volumes of the compartments (Kora et al. 2019).

335



340

Figure 1. Schematic diagram of compartmentalizing tree measurements for the non-destructive sampling of tree volume. Taken from Picard, Saint-Andre, and Henry (2012).

Non-destructive determination of tree volume can also be achieved through imaging technologies, in which scaled 3-D models can be used to digitally calculate the tree volume. This can be done with passive imaging such as photogrammetry (Bauwens et al. 2017) or active imaging such as LiDAR (Karpina et al. 2016). Depending on the species under investigation, the line of sight to the stems and trunk, which can be blocked by the leaves, can be problematic.³

345

³ In preparation for this present study, we did an initial experiment with using photogrammetry to obtain an estimate of tree volume using structure-from-motion photogrammetry to generate a volumetric estimate;

In order to convert volumetric measurements to biomass and/or total carbon, measurements of wood and carbon density are needed. Wood and carbon density vary by species, age and environmental factors when examining separate trees (Burdon et al. 2004), but also vary within each tree, with different values for the different plant parts and even the same plant parts of different sizes. For instance, an increase in diameter is typically accompanied by a change in both the wood density (mass per unit volume) and the density of carbon within the wood (Picard, Saint-Andre, and Henry 2012). Typically, general wood/carbon densities are determined for classes of woody material through sampling and analysis. The volume of each woody type is then multiplied by the average density of that woody type to determine the total biomass and carbon density for each category.

2.3. Methods

2.3.1. Overview

To develop an allometric equation for *A. altilis* in Hawai'i and assess the appropriateness of other published allometric equations, this project collected detailed architectural measurements to estimate the total volume of standing unadulterated breadfruit trees, and collected wood and leaf samples from trunks and stems of various diameters. Between August 2020 and March 2023, 12 breadfruit trees of the cultivar 'Maoli' were opportunistically sampled on Hawai'i Island. Detailed architectural data was collected in accordance with the procedures used in other minimally destructive study methods (Kora et al. 2019; Picard, Saint-Andre, and Henry 2012), in which diameter measurements were collected every 1m along all woody material of the entire tree. Wood samples were collected from branches of varying diameters from four trees and were used to calculate the wood density and carbon density, which were subsequently used to generate linear regression relationships against branch diameter. These relationships were integrated with the tree volume model for each individual segment based on the average stem diameter of each section in order to calculate total stem biomass and carbon. Foliar mass and carbon were obtained by collecting terminal branches of various sizes from eight trees. Leaf biomass was determined for all leaves on the branch and regressed against terminal branch base diameter. A simple mathematical model was created in Excel (Microsoft; Redman, WA) to integrate all measurements and calculate the total volume, biomass, and carbon associated with each tree.

2.3.2. Woody Biomass Volumetric Estimation

The major and minor diameters were measured and recorded every meter along the main trunk and all the branches of each tree, starting at the ground surface and each branch junction. For terminal measurements, the length of the final segment was recorded along with the branch diameter 5 centimeters from the terminus. The major and minor elliptical diameters were measured using tree calipers to the nearest mm, and the length of each segment was measured with a cloth measuring tape to

however, the broad leaves of *A. altilis* challenged development of an acceptable point cloud due to line of site issues.

380 the nearest cm. For each individual branch, the tree ID, branch number, and segment number were recorded.

2.3.3. Wood Density and Carbon Content

To determine wood and carbon density, “cookies,” or cross sections of branches, of various diameters were opportunistically collected where destructive sampling was possible. The volume of the wood cookies was determined using the water displacement method, and the samples were then oven-dried at 100°C until constant mass was achieved. Wood density for each cookie was then calculated by dividing dry mass by volume. Cross sections were drilled out of the cookies, and the dried samples were pulverized, encapsulated, and analyzed for total carbon concentration using an Elemental Analyzer. Wood and carbon density were regressed against the average radius of each cookie to describe wood density and carbon as a function of stem diameter.

2.3.4. Foliar Biomass Estimation

Forty branches of varying base diameters were harvested from trees, and the base and terminal diameter of each branch were measured and recorded. All leaves from each branch were removed at the base of the petiole, oven-dried and weighed. Regression analysis was used to explore the relationship between foliar biomass and terminal branch diameter. Half of the leaf samples were pulverized, encapsulated, and analyzed for total carbon concentration using an Elemental Analyzer.

2.3.5. Statistical Analysis

Linear and non-linear regressions were used to examine the relationship between parameters of interest. Analyses were conducted using JMP (SAS Institute; Cary, NC), with the coefficient of determination (r^2) and probability values (P) used to describe the accuracy of the mathematical equations (Kora et al. 2019). A simple Excel model was used to combine all factors measured and compute total volume, biomass and carbon for each tree measured. For each branch segment measured, the volume was calculated based on a conic stem shape as described in Equation 1.

Equation (1)
$$V = \frac{\pi(\frac{D_x}{2})^2 + \pi(\frac{D_{x+1}}{2})^2}{2} \times L$$

405 Where V is the volume in cm^3 , D_x and D_{x+1} are the diameter at the upper and lower bounds of the segment, and L is the length of the segment, all measured in cm.

For each segment, the regression equations describing the relationship of wood density and carbon concentration were applied to the average diameter of the segment, so that total carbon density was considered a continuous function of branch diameter, as in Equations 2-4.

410 Equation (2)
$$C_{wg} = V * \rho * C_{\%}$$

Equation (3) $\rho = f\left(\frac{D_x + D_{x+1}}{4}\right)$

Equation (4) $C_{w\%} = f\left(\frac{D_x + D_{x+1}}{4}\right)$

Where C_{wg} is the total carbon mass of woody components in g, ρ is the wood density in g/cm^3 , and $C_{w\%}$ is the woody carbon concentration.

415 For each branch, total leaf biomass was calculated by applying the determined regression equation to the base diameter of each branch, with total carbon calculated as the product of leaf biomass and the average leaf carbon density, as in Equations 5 and 6.

Equation (5) $C_{lg} = C_{l\%} * M_l$

Equation (6) $M_l = f(D_b)$

420 Where C_{lg} is the total carbon mass of leafy components in g, $C_{l\%}$ is the average carbon concentration in breadfruit leaves, M_l is the biomass of the leaves in g, and D_b is the base diameter of a terminal branch.

Total woody and leaf biomass was calculated in Excel for each segment. In the case of leaves, the biomass was only calculated for “Segment 1” of each branch to capture the base diameter of each branch. Total tree biomass and total tree carbon were calculated as the sum of all individual woody

425 segments and leaf components. This process is represented schematically in Figure 2.

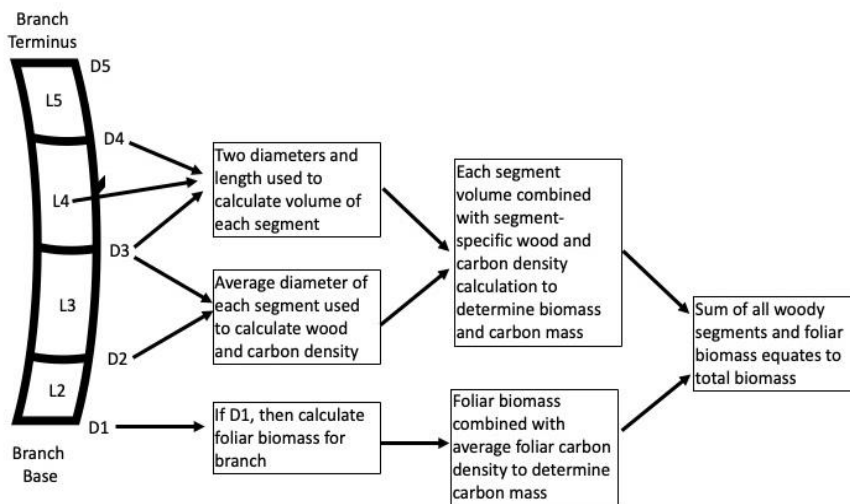


Figure 2. Conceptual diagram illustrating the simple spreadsheet model used in this study to calculate the total biomass and carbon mass of each tree.

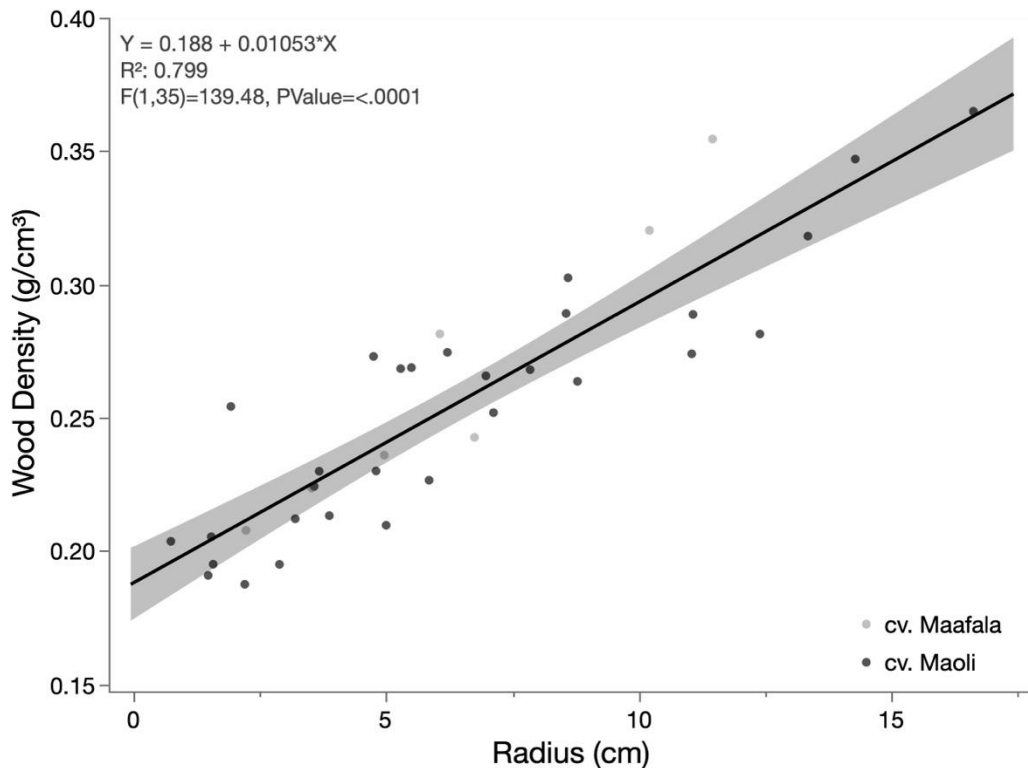
430 Total tree biomass and carbon were separately compared against tree DBH, and a non-linear regression fit was used to characterize the relationships.

2.4. Results

2.4.1. Wood Density and Carbon Density

435 Cross-section “cookies” from 37 branch samples ranging in average radius from 0.7375 cm to 16.625 cm were harvested and measured from four ‘Maoli’ and one Ma’afala’ tree. Wood density exhibited a generally linear increase with increasing radius of the branch/trunk (Figure 3). The relationship between wood density as a function of branch radius is fairly robust ($r^2 = 0.799$). Although only a single ‘Ma’afala’ tree was sampled, the two cultivars do not appear to differ substantially. The relationship of wood density to average radius, shown in Equation 7, was used to replace the generic function outlined in Equation 3.

440 Equation (7)
$$\rho = 0.188 + 0.01053 \times \frac{D}{2}$$



445 **Figure 3. Linear regression of the dry wood density against the radius of 37 wood “cookies” opportunistically collected from ‘Ma’afala’ and ‘Maoli’ cultivars of breadfruit via destructive sampling.**

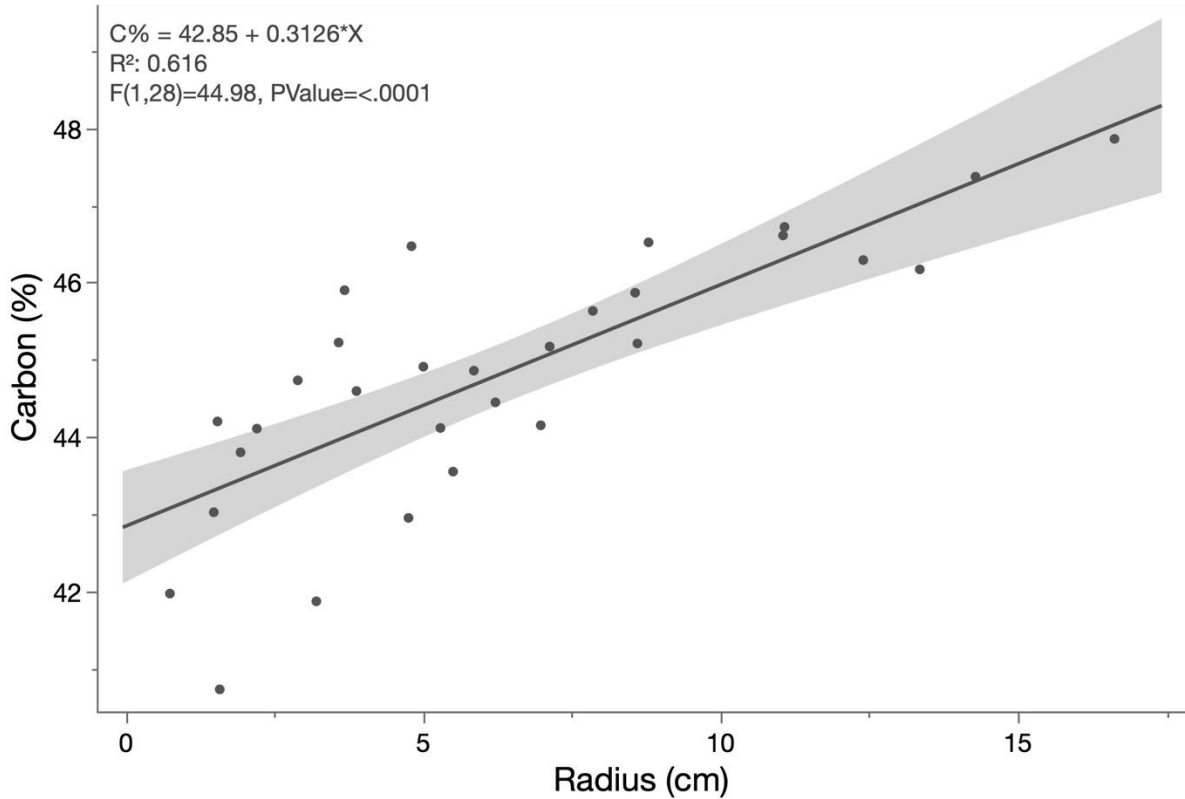
445

Percent Carbon (%C) was determined for the branch cross sections of the Maoli variety only. The mean for all samples was 44.8 %C with a standard deviation of 1.7 and standard error of 0.3. Percent carbon as a function of branch radius demonstrated a slight increase with branch diameter (Figure 4). Although the relationship appears to have some non-linear behavior, the application of various non-linear regressions only marginally improved the r^2 values, due to the reasonably high variation in lower radius samples. The

450

linear relationship used to describe the carbon concentrations as a function of average radius, shown in Equation 8, was used to replace the generic function outlined in Equation 4.

Equation (8)
$$C_{w\%} = 42.85 + 0.3126 \times \frac{D}{2}$$



455 **Figure 4. Linear regression of percent carbon as a function of stem radius for 30 branch cross sections opportunistically collected from ‘Maoli’ breadfruit cultivars on Hawai‘i Island.**

In spite of differences in percent carbon by variety, bringing wood density and percent carbon into a carbon density function (gC/cm³) by average radius yields a highly significant (P<0.0001) relationship with a relatively more robust r² (0.826). Describing varietal gC/cm³ yields a more robust r² for both the Ma‘afala‘ variety (r² = 0.908) and for the Maoli variety (r² = 0.858; Figure 5).

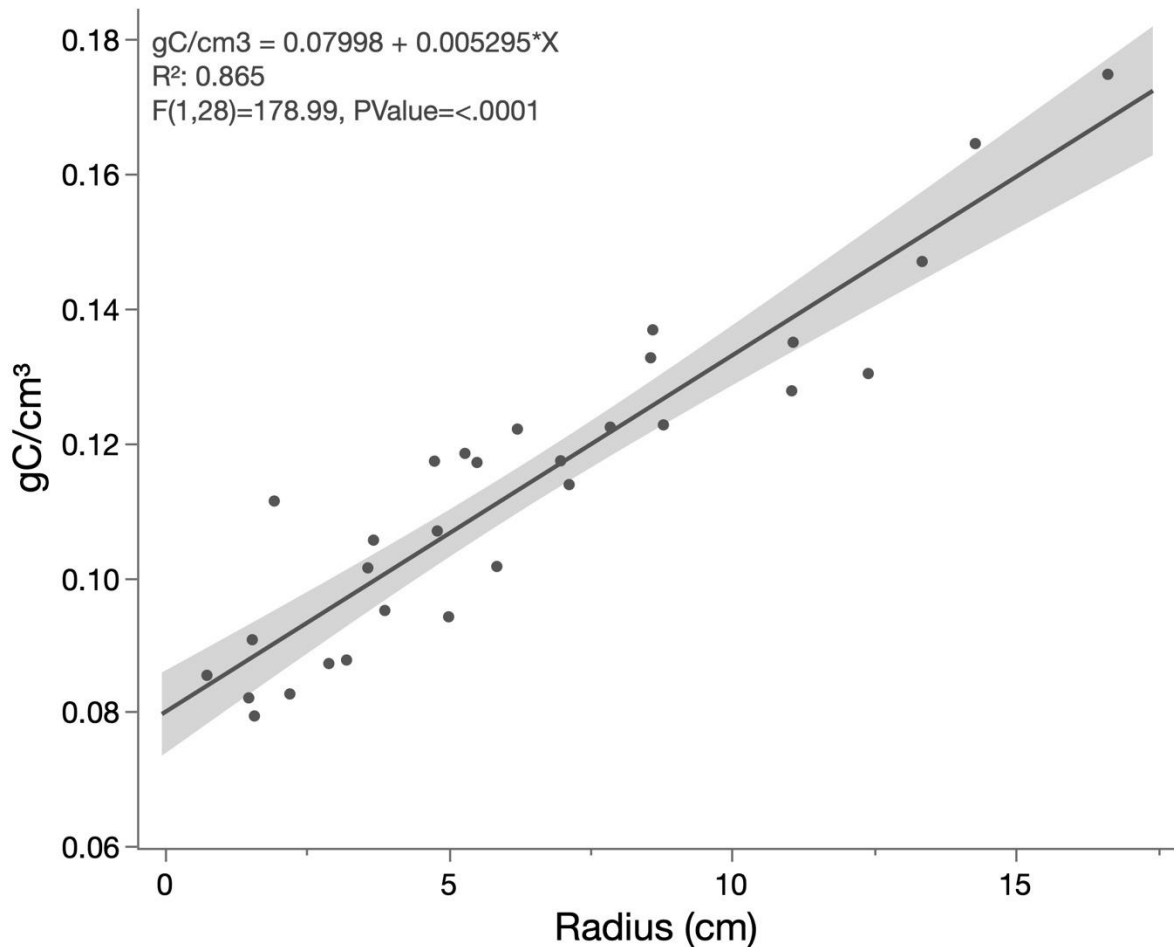


Figure 5. Linear regression of carbon density (gC/cm³) as a function of stem radius for 30 branch cross sections opportunistically collected from 'Maoli' breadfruit cultivars on Hawai'i Island.

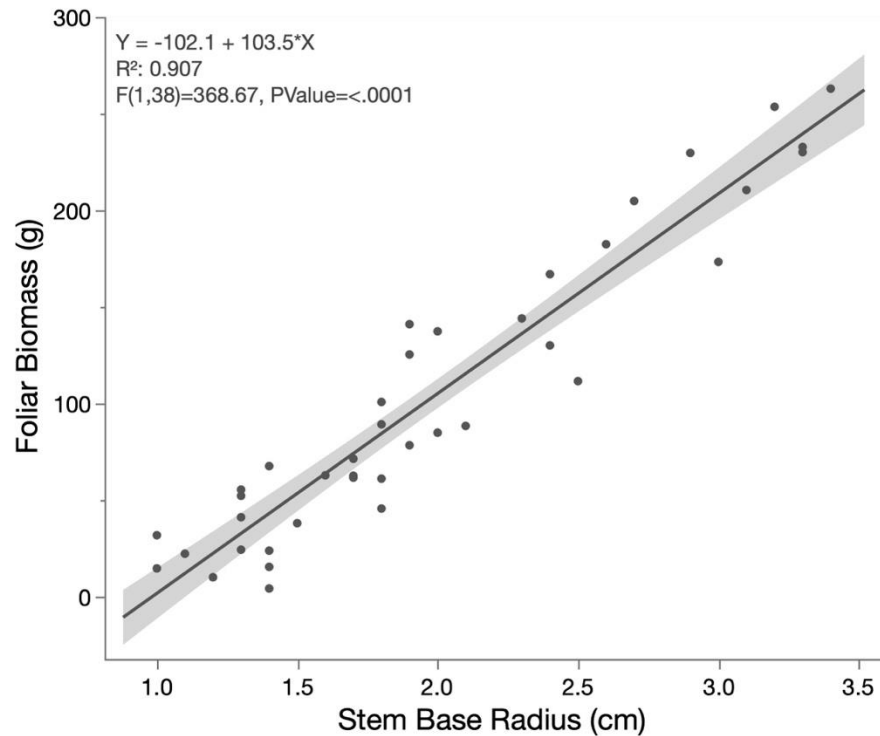
465

2.4.2. Foliar Biomass

Foliar biomass for 38 branches was determined and described as a function of stem diameter. The total number of leaves per terminal branch ranged from 4 to 14 with total dry weight ranging from 3.96 g to 262.85 g. Dry foliar biomass was more strongly correlated with base stem diameter (Figure 6; $r^2 = 0.907$) than top stem diameter ($r^2 = 0.819$). The associated regression equation used to describe leaf biomass as a function of terminal branch base diameter, shown as Equation 9, was used to replace the generic function outlined in Equation 6.

475 Equation (9)
$$M_l = -102.1 + 103.5 * \frac{D}{2}$$

Carbon percentage for the foliar biomass was determined for half (19) of the samples and found to have an average of 51.4% with a standard deviation of 1.14.



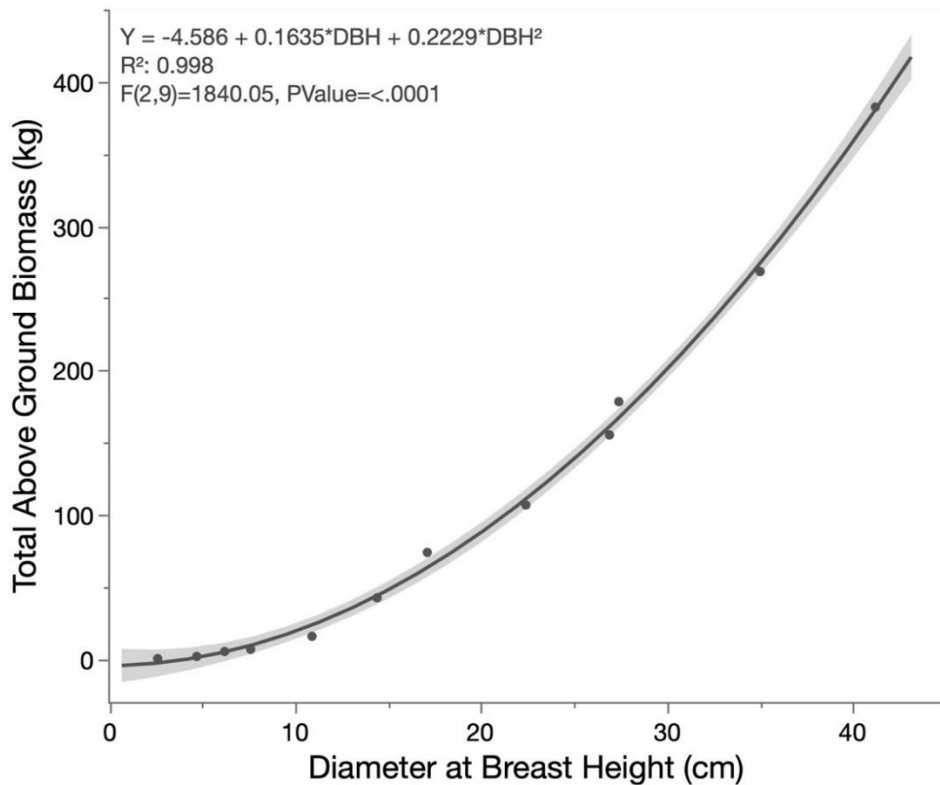
480 **Figure 6. Foliar biomass as a function of terminal branch stem radius for 38 individual branches harvested from the ‘Maoli’ breadfruit cultivar on Hawai‘i Island.**

2.4.3. Woody Biomass Volume

Using the method described, volumetric measurements of the above ground woody components of 12 *A. altilis* ‘Maoli’ trees from Hawai‘i Island ranging in DBH from 2.6 cm to 41.2 cm were determined. Using a simple spreadsheet model, the total woody biomass and foliar biomass were calculated for each tree, as surmised in Table 3. Total ABG for each tree was regressed against the measured DBH of those trees, demonstrating a robust non-linear relationship (Figure 7), which served as a preliminary allometric equation for breadfruit trees in Hawai‘i, described in Equation 10.

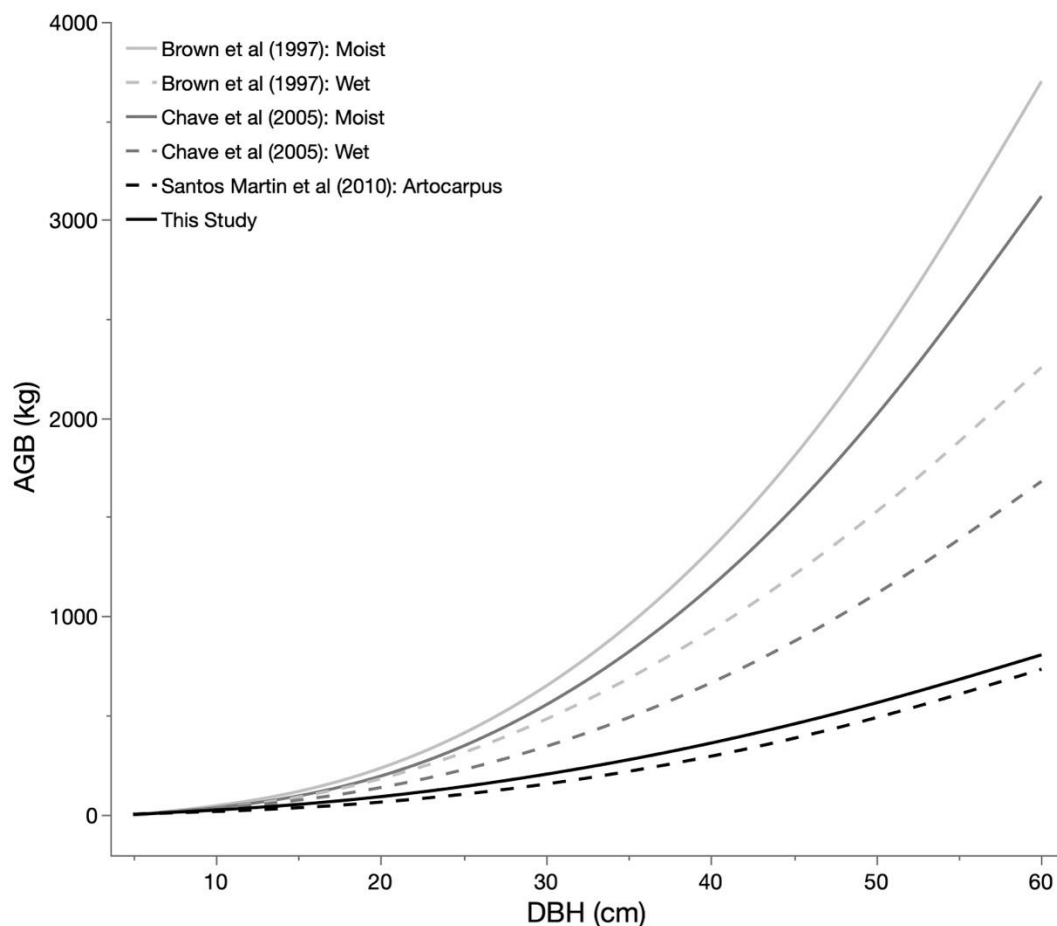
490 Equation (10)
$$ABG = -4.586 + 0.1635 \times DBH + 0.229 \times DBH^2$$

Table 3. Woody, foliar, and total above-ground biomass for 12 breadfruit trees on Hawai'i Island as determined through detailed architectural measurements and a simple spreadsheet model.				
	DBH	Dry Wood Biomass (kg)	Dry Leaf Biomass (kg)	Total AGB (kg)
Tree 1	10.9	11.971	3.851	15.822
Tree 2	17.1	59.815	14.139	73.955
Tree 3	2.6	.216	.177	0.393
Tree 4	7.6	5.510	1.287	6.807
Tree 5	35	232.102	36.394	268.496
Tree 6	27.4	144.833	33.566	178.398
Tree 7	41.2	350.608	31.811	382.419
Tree 8	6.2	4.446	.854	5.300
Tree 9	4.7	1.575	.324	1.899
Tree 10	14.4	32.452	10.054	42.506
Tree 11	26.9	124.470	30.854	155.324
Tree 12	22.4	83.629	23.186	106.814



500 *Figure 7. Quadratic regression of total above ground biomass (AGB) against diameter at breast height (DBH) for 12 unadulterated breadfruit trees on Hawai'i Island.*

In comparison to previously published allometric equations, as shown in Figure 8 below, the relationship from this study aligned closely with the equation derived from the destructive sampling of jackfruit by Santos Martin et al. (2010) and is more conservative than all the pan-tropical equations except for the Chave Wet equation.



510 **Figure 8. Graphical comparison of the allometric equation determined in this study alongside four relevant pantropical allometric equations and the one published allometric equation identified for an Artocarpus species. The equation calculated in the present study closely aligns with the Santos Martin et al. (2010) for jackfruit, both of which are well below the four pantropical equations.**

515 **2.5. Discussion**

Even within a single species, local variation can impact tree parameters and cause significant disruption to the fit of an allometric model. To effectively account for this local variation, sampling adequate trees to develop a tailored allometric equation is necessary, but not feasible for most operations. This study demonstrates that minimally destructive methods that incorporate wood and carbon density measurements can enable the development of allometric equations that approximate destructively

derived equations. The robust nature of the relationship was surprising, but this is perhaps because all of the trees sampled were from open areas where the trees could grow unadulterated and without competition.

525 The results presented earlier demonstrate potential variation in wood density and carbon density. The application of wood and carbon density as a continuous function of branch diameter, as opposed to the more standardized approach of classifying woody material into types and applying average values, may improve estimates of total carbon, and should be explored further as a standardized method for carbon accounting. The incorporation of a continuous relationship was afforded because of the non-destructive
530 methods employed, which required the tedious measurements of all branch diameters, as opposed to destructive sampling that tends to not record branch diameters throughout the entire tree. However, as imaging methods become increasingly improved and are applied more frequently the opportunity to do mathematical integration will also increase. Therefore, while some may argue that non-destructive sampling is less robust than complete destructive sampling of trees, here it is demonstrated that non-
535 destructive methods also afford new opportunities to improve the accuracy of total carbon calculations.

Our resulting allometric equation aligns well with the only other equation published for an *Artocarpus spp.*, suggesting the reality of *Artocarpus* AGB fall within this range. These values are considerably lower for the generic pan-tropical equations for broadleaf species. This makes sense, given that breadfruit is well known as a “light” wood, being used in traditional Polynesian culture for its lightness and ability to float.
540 Breadfruit was therefore used to make fishing floats, the gunnels on canoes, and surfboards because of its characteristics. The “lightness” of the wood corresponds to a lower wood density and, accordingly, a lower carbon density on a per volume basis.

We did not attempt to incorporate height or other canopy measurements, and Goodman et al. (2014) highlights that the influence of crown diameter and canopy characteristics have not been well studied nor
545 incorporated into existing allometric equations (Goodman, Phillips, and Baker 2014). As trees grow and compete for access to light, a potentially significant relationship develops between crown expansion and AGB; once outside the confines of an understory trees tend to expend resources to grow more horizontally than vertically. This change in growth pattern may impact the accuracy of allometric equations that do not account for canopy architecture. These findings apply to the present analysis as
550 breadfruit trees often grow in the open where exposure to more sunlight is often associated with larger canopies (Zhou et al. 2015). In addition to a larger canopy architecture, in general, open-grown trees often have more significant tapers, and higher bole specific gravity; these factors could lead to over or underestimates in AGB when using forest-derived allometric equations (Zhou et al. 2015). Future work could test the development of more sophisticated, non-destructive models that incorporate height and
555 other aspects of canopy architecture in addition to sampling for differences in varieties, which may become particularly relevant when monitoring trees in orchard settings that are routinely pruned.

CHAPTER 3. GROWTH RATES OF *A. ALTILIS* AND LANDSCAPE SCALE CARBON IMPLICATIONS

3.1. Introduction

560 This chapter builds upon the allometry developed in Chapter 2 to further extrapolate outcomes across
time and space. The development of the relationship between diameter at breast height (DBH) and total
above-ground biomass (AGB) and carbon has implications at the landscape scale, particularly when
considering potential carbon policies. Specific survey techniques are required when using allometry to
565 estimate carbon at the stand or forest level (Picard, St. Andre and Henry 2012), and employing the
allometric equation to explore biomass and carbon of a current *A. altilis* orchard lies beyond the scope of
this project; however, the data collected here, when combined with growth data allows for the estimation
of how much carbon is potentially contained within a given landscape at various points in the growth and
development of planned agriculture projects over time.

570 Additionally, a robust AGB allometric equation can potentially enhance the below-ground biomass (BGB)
estimates. BGB allometry faces even more substantial challenges than the development of AGB
allometry in that the tree's entire root structure must be carefully excavated, weighed and measured in a
manner similar to the destructive sampling required for the development of AGB allometric equations.
Therefore, forestry and carbon projects often rely on root-to-shoot ratios to estimate the BGB based on
575 the AGB estimate; better above ground allometry, such as the work from the previous chapter, may by
extension, lead to a better estimate of below ground biomass. Mokany et al. (2006) built the standard
reference table for root-to-shoot biomass after review of 786 estimates from 266 sources that
characterized the root-to-shoot ratio from across the biomes of the earth. (Mokany, Raison, and
Prokushkin 2006).⁴ By applying BGB estimates, it is possible to estimate the total *A. altilis* biomass and
carbon associated with the active, vegetative portion of a tree.

580 Furthermore, the rates of accumulation and total stocks of carbon can be estimated by relating the growth
of breadfruit over time to the tree parameter that drives the allometry; that is, DBH. To continue to
develop support for the application of breadfruit as a climate-smart commodity, this analysis applies the
allometric equation developed previously to begin to develop a landscape scale estimate of carbon. The
two objectives of this section of the thesis are to (1) develop a model of breadfruit growth in DBH over
585 time; (2) use our growth and allometric equations to extrapolate the landscape-level carbon sequestration
potential of breadfruit biomass by applying published BGB information and industry standards.

⁴ When discussing terrestrial carbon pools, root shoot ratios are a method utilized by carbon accounting. However, more advanced concepts such as Total Below Ground Carbon Flux (TBCF) and Below Ground Net productivity (BNPP) better describe the flow of carbon through the terrestrial system. BNPP in particular better connects the carbon plants utilize in the root system to the development of soil carbon. Describing carbon pools are the focus of this thesis; therefore, the thesis will focus on root shoot ratio leaving discussions of BNPP for future work.

3.2. Background

590 3.2.1. *Describing Growth of DBH over time*

Developing equations to describe changes to tree diameter as the tree grows is one of the fundamental purposes of tree growth models; calculating this change over time is needed to estimate the accompanying biomass volume growth (Hann and Larsen 1991). As with biomass allometry, a variety of variables may be included in the DBH growth equation, such as canopy characteristics and height. Many
595 of these decisions are based on the intended purpose of the equation. Growth equations have a variety of uses including estimating basal area per hectare and other stand characteristics.

Environmental parameters are important in terms of plant growth, with a wide range of factors being influential in plant growth including temperature, soil type and fertility, rainfall and water availability, solar radiation, and many others (Cienciala et al. 2016). Typically, the most limiting factor is considered to
600 define the rate of tree growth, and habitat modeling for breadfruit and other trees tends to take the approach of understanding the most limiting environmental parameter (Mausio, Miura, and Lincoln 2020) . However, different factors may be limiting across different time periods, both within annual cycles and across inter-annual variation (Yang et al. 2022). Typical protocols for determining tree growth rates involve measuring the desired tree parameters over time. However, space-for-time substitution may be
605 used if trees of multiple ages are accessible to be measured.

3.2.2. *Belowground Biomass (BGB)*

As described earlier, a portion of the radiant energy intercepted by the plant is directed to above-ground biomass (AGB). In addition to above-ground allometry, trees and plants also dedicate a portion of their biomass below ground in accordance with a root-to-shoot ratio. Below-ground biomass (BGB)
610 encompasses the biomass of live roots >2 mm diameter that includes the coarse roots of trees, shrubs and other living plants. Similar difficulties challenge the precise measurement of BGB that challenges AGB. Therefore, root-to-shoot ratios are frequently used to predict the structural biomass of the tree/forest that lies below ground (IPCC 2019). Table 4, taken from Chapter 4 of the 2019 IPCC Guidelines for National Greenhouse Gas Inventories, captures the work of Mokany et al (2006).

615

Ecological Zone	Above Ground Biomass	Ratio
Tropical Moist Deciduous Forest	AGB < 125 tons ha ⁻¹	.20
	AGB > 125 tons ha ⁻¹	.24
Tropical Dry Forest	AGB < 20 tons ha ⁻¹	.56
	AGB > 20 tons ha ⁻¹	.28
Subtropical Humid	AGB < 125 tons ha ⁻¹	.20
	AGB > 125 tons ha ⁻¹	.24
Subtropical Dry	AGB < 20 tons ha ⁻¹	.56
	AGB > 20 tons ha ⁻¹	.28

620

3.3. Methods

3.3.1. Tree Growth Evaluation

To determine a growth equation for *A. Altilis*, DBH was measured for 208 trees where known or approximate ages could be supplied by the tree owners. Tree locations were recorded and used to extract the modeled habitat suitability of breadfruit based on geospatial modeling by Mausio et al. (2020). Mausio et al. (2020) used a fuzzy-set methodology based on the distribution of 1,200 naturalized breadfruit trees across the Hawaiian archipelago to create a habitat suitability score of 0-100 based on environmental parameters of rainfall, temperature, solar radiation, soil pH, and soil class. Their model was validated using production data from 56 producer sites across the state. Due to the relatively small sample size in this study, suitability scores were converted to categorical representations of breadfruit suitability as High (Suitability >81), Medium (70 < Suitability < 81), and Low (Suitability < 70).

630

Linear and non-linear regressions were used to examine the relationship between tree age and DBH across all samples and by suitability class using JMP software (SAS Institute; Cary, NC), with the coefficient of determination (r^2) and probability values (P) used to describe the accuracy of the mathematical equations (Kora et al. 2019).

635

3.3.2. Extrapolation of Landscape-scale Carbon Sequestration in Breadfruit Biomass Over Time

A growth equation is applied to determine projected tree DBH at 5, 10, 15, and 20 years. For extrapolations in this study, we employ the best-fit relationship between age and DBH for the high-suitability classification, assuming that high-suitability sites would be preferentially developed for any large-scale projects. Using the allometric equation and %C model generated in the previous chapter, DBH is used to estimate AGB, as well as total above-ground carbon. From AGB, BGB is estimated based on the published root-to-shoot ratio, to which a generic carbon concentration is applied to estimate total below-ground carbon in the biomass. The summation of total above- and below-ground carbon will provide an estimate of total tree carbon at each timepoint. To move to the landscape scale, we use the Hawaii Ulu Cooperative's guidelines of a planting density of 125 trees per hectare to create an estimate of total carbon stocks accumulated in the breadfruit biomass and the carbon dioxide equivalent. An exercise

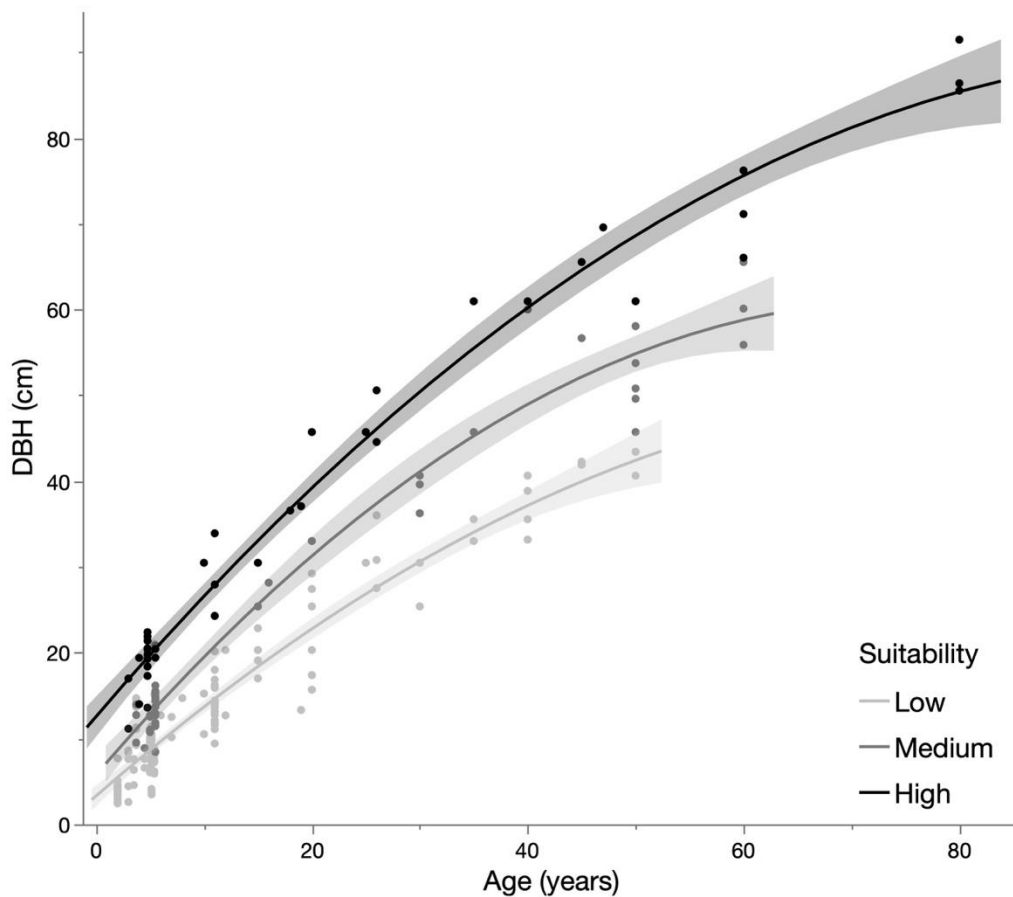
645

of error propagation through the root mean square errors is conducted to understand the 95% confidence interval associated with the final estimates.

650 3.4. Results

3.4.1. Growth

The DBH and age of 208 *A. altilis* trees from the Big Island of Hawaii were recorded, and habitat suitability was determined in ArcGIS by extracting the locational data from the suitability map generated by Mausio et al (2020). 95 Trees were Hawaiian variety and 113 were of the Maafala variety. Across all trees, the linear regression of diameter against age was indistinguishable between the two varieties, and subsequent analysis combined the two varieties. Trees were broken into suitability classes of High ($n=38$), Moderate ($n=42$), and Low ($n=128$). Using JMP software, we regressed DBH against age by applying suitability classification. Growth curves were best explained by a quadratic function (Figure 9) with the resulting equations presented in Table 5.



660 **Figure 9. Quadratic regression of DBH against age for 208 breadfruit trees on Hawai'i Island as**
665 **classified by habitat suitability.**

Suitability Class	Equation	R²	RMS Error
High	DBH = 12.57+1.474(Age) – 0.007044(Age) ²	.98	3.8
Medium	DBH = 5.766 + 1.471(Age) – 0.009793(Age) ²	.96	3.6
Low	DBH = 3.308 + 1.066(Age) – 0.005585(Age) ²	.89	3.3

3.4.2. Landscape Scale Carbon Estimate

Only the high suitability class was used for extrapolation, assuming that areas of high suitability would be preferentially developed for breadfruit industry, as noted in Equation 11.

670 Equation (11) $DBH = 12.57 + 1.474(Age) - 0.007044(Age)^2$

The growth formula was used to estimate DBH of trees at ages 5, 10, 15 and 20 years. The resulting DBH values were plugged into the allometric equation developed in the last chapter, as shown in Equations 12 and 13 below.

Equation (12) $AGB = -4.586 + 0.1635 \times DBH + 0.2229 \times DBH^2$

675 Equation (13) $kgC = 2.25 - 0.8715 \times DBH + 0.1172 \times DBH^2$

A root-to-shoot ratio of 0.56 was applied to the resulting AGB using the generic conversion for dry-subtropical environments as published by Mokany et al (2006) to estimate breadfruit BGB per tree over time, multiplied by a generic carbon concentration of 44.8%. To extrapolate to a per hectare basis we apply the industry standard of 50 trees per acre, or 125 trees per hectare based upon a 30-foot planting spacing and convert to the CO₂ equivalent by multiplying by the ratio of molecular weight of carbon to Carbon Dioxide (44:12). The extrapolations are summarized in Table 6.

680

Age	DBH (cm)	AGC (kg/tree)	BGC (kg/tree)	Total C (kg/tree)	CO₂ (mt/ha)
5	19.76	39.2	9.2	48.4	22.2
10	26.61	73.3	16.9	90.2	41.3
15	33.10	115.0	26.3	141.2	64.7
20	39.23	162.9	37.0	199.8	91.6

3.4.3. Error Estimates

685 The extrapolation in the previous section relies on multiple relationships, each of which has a degree of error associated with it. This includes our allometric equations and sub-relationships, the growth equations, and the generic BGB estimates applied.

In general, there are four major sources of error in estimating AGB including sample tree selection, tree measurement, statistical modeling and application of the statistical model (Cunia 1965). In this section, 690 we will briefly describe the error associated with our statistical model.

To develop our allometric model of *A. altilis* AGB we employed two sub-models: 1) the relationship of stem diameter to wood and carbon density and 2) the relationship of stem diameter to foliar biomass. These sub-models fed into the final allometric model. As described earlier, we did not begin with a geometrical argument as described elsewhere (Chave et al. 2005) but instead followed the methods 695 outlined in Picard, St. Andre and Henry (2012).

Table 7. Root Mean Square Error of Associated Models. Errors associated with the regression relationships that fed into the allometric equations as well as the final allometric equation.

	Dry Density to (g) Stem Diameter (cm)	Foliar Biomass (kg) to Bottom Stem diameter (cm)	AGB (kg) to DBH (cm)	DBH growth rate
R²	.799	.904	.998	.98
Root Mean Square Error	.021 g/cm ³	23.516 g	6.699 kg	3.8 cm

3.5. Discussion

700 Utilizing tree age and habitat suitability, strong relationships between age and DBH were shown, suggesting that good predictions about growth rates across environments can be determined for breadfruit. Such relationships to habitat quality have been shown to relate to both the productivity and the quality of the fruit produced (Erland et al, 2023; Needham, Jha, and Lincoln 2020). The growth rates were utilized in conjunction with our previously determined allometry, published root-to-shoot ratio, and industry 705 standards to demonstrate a landscape-level prediction of carbon content within the biomass associated with breadfruit orchards. It is important to note that trees sampled for both the growth rates and the determination of AGB were unadulterated trees. This is unlikely for an orchard scenario, in which trees are generally pruned and otherwise actively managed. This could both increase (e.g. through fertilization) or decrease (e.g. through pruning) growth rates, and would likely decrease AGB (through pruning).

710 Additionally, this study did not sample root material nor engage in a thorough assessment of the contribution of roots to the carbon estimate. Future work could also better describe how carbon percentage varies over time and by variety. This would make the carbon estimate more robust and could point to ways of better designing carbon projects. These are all activities that need to be considered in future work. However, this initial analysis demonstrates the potential to provide reasonably accurate 715 assessments and predictions of breadfruit growth and carbon storage.

CHAPTER 4. SENESCENCED ORGANIC MATTER POOL (LITTER)

4.1. Introduction

720 Litter lies at the transition point in the flow of carbon in the terrestrial ecosystem between above-ground biomass and between a return of carbon to the atmosphere or incorporation into soil organic matter. Of the major broad categories of terrestrial carbon, the litter is among the most ephemeral, with residence times of some components as short as days. The uncertainties associated with estimates of the rate of transfer from dead organic matter to the soil organic carbon pool or emission back into the atmosphere
725 are generally high (IPCC 2019).

Because of the relatively small size, short duration, and highly variable kinetics of litter decomposition, the IPCC guidelines provide significant leeway to make assumptions or otherwise minimize the effort expended to quantify this pool and its associated flows (IPCC 2019). Further, IPCC guidelines highlight that the dead organic matter pool is not likely to fill a “key category role” meaning, that the category is not
730 likely to have a significant effect on the total inventory (IPCC 2019).

A carbon accounting methodology published by Verra—a non-profit and world leader in setting standards for carbon project accounting—continues the theme of minimizing the importance of the litter pool because of its small contribution. However, if project planners have reason to believe that the pool is significant, Verra drafted an Improved Agriculture Land Management methodology that describes
735 methods for quantifying litter based on the Clean Development Mechanism. Based on how the carbon accounting standards approach this carbon pool, a first step is to assess the importance of this pool’s carbon contribution to the overall total Carbon of the system. The objective of this study is to provide a characterization of the significance of litter in the overall carbon accounting of breadfruit orchard systems.

4.2. Background

740 As described in the AGB estimate chapter, trees dedicate a species-specific amount of energy to biomass production in general, and leafy biomass in particular. For most species, senescence, or litterfall, is a part of a natural cycle of growth and development. Studies have characterized the litterfall rate for a number of *Artocarpus spp.* One study observed a litterfall rate of 13.76 kg/ha⁻¹ (Das and Das 2010) in *A. chama* species, while another study observed approximately .5 Mg ha⁻¹ in both *A. heterophyllus* and *A. hisutus*
745 (Jamaludheen and Kumar 1999). In addition to the natural senescence process, breadfruit orchards would also need to account for annual pruning and associated management techniques.

As litter falls, the rate at which it decomposes and transitions to other pools is highly dependent on litter characteristics such as carbon-to-nitrogen ratio and lignin content, and based on microclimate conditions, microbes, and earthworms under the canopy (Tangjang et al. 2015).

750

Table 8. Litter characteristics of *Artocarpus* spp. from published studies.

Species	Litterfall Rate (kg/ha ⁻¹)	C:N Ratio	Lignin Percentage (%)	Author
<i>Artocarpus chama</i>	13.76	43.58	N/A	Das and Das 2010
<i>Artocarpus heterophyllus</i>	N/A	32.44.	N/A	Das and Das 2010
<i>Artocarpus heterophyllus</i>	N/A	27.65	17.48	Tangjang et al. 2015
<i>Artocarpus heterophyllus</i>	N/A	N/A	15.18	(Isaac and Nair 2006)
<i>Artocarpus hisutus</i>	N/A	N/A	28.7	(Isaac and Nair 2006)
<i>Artocarpus heterophyllus</i>	~500	N/A	17.9	Jamaludheen and Kumar 1999
<i>Artocarpus hisutus</i>	~500	N/A	31.4	Jamaludheen and Kumar 1999

Anecdotaly, agroforestry farmers in India report that *Artocarpus spp* leaves decompose more slowly than other trees in the agroforestry system because of their thickness and large size (Ashesh 2010). This fits with findings that the decay rate for wild jackfruit (*A. hisutus*) is lower than for other tropical trees (Issac 2004). Issac (2004) observed that *A. hisutus* decomposition was a first-order process with a half-life of 9.45 fortnights, and that after 17 fortnights under the canopy, 95% of the litter material had decomposed (2004). In general, studies have described the decay of *Artocarpus* litter as a bi-phasic, first-order process with a decay constant (k) between 2 – 4 units of mass per time. However, this process remains poorly understood, and the specific kinetics of carbon flows into the soil carbon pool or back into the atmosphere are influenced by a number of difficult-to-quantify factors (IPCC 2019).⁵

4.3. Methods

As shown in Figure 9, to assess the standing litter stock, a 20 cm by 20 cm cardboard square was placed on the accumulated litter material under the canopy of six randomly selected trees at the Southern Turf, in Central Oahu, which is a commercial breadfruit orchard established in 2013. The four sites were situated randomly at the mid-canopy of each tree. Using a knife, the litter material within these four 20x20 cm squares were separated from the adjoining dead organic matter and collected into a paper sample bag. Measurements were also taken from the trunk of each tree to the edge of the litter field to estimate the total area associated with litter material.

⁵ Further, a growing body of literature points to roots and soil microbial communities as the largest contributors to soil carbon, not AGB dead organic matter.



770

Figure 9. Illustration of the litter sampling, showing an example of the four 20 cm² collection areas, with the dashed line representing a measurement of the radius of the litter field.

At the lab, the harvested leaf and coarse woody material were dried at 60 °C, from which dry weights of
775 the total harvested material were calculated. The dried dead organic matter material was separated into
coarse woody samples and leaf material samples. These leaf and wood samples were homogenized
separately with a ball mill (Retsch MM200 mixer mill; Retsch GmbH, Haan, Germany) to pass through a
250-ml sieve, and the C and N concentrations were determined by oxidative combustion on an elemental
780 analyzer (Costech ECS 4010 CHNSO Analyzer; Costech Analytical Technologies Inc., Valencia, CA,
USA).

4.4. Results

4.4.1. Layer of Surface Litter Characteristics

Samples and measurements of the layer of surface litter from six trees at Southern Turf in Central Oahu
785 were collected. The mean layer of surface litter area was 19.84 m² per tree, with a standard deviation of
6.57 m².

4.4.2. Litter Mass and Carbon Percentage

With four samples collected from each tree, a total of 24 litter samples were collected from six trees at
Southern Turf. As described above, in the lab these samples were homogenized into leaf litter and wood
790 litter samples for each tree and these samples were sent for total carbon analysis. Mean leaf litter mass
per homogenized sample was 241.07 g with a standard deviation of 89.4 g, and mean wood litter mass
per homogenized sample was 41.43 g with a standard deviation of 26.15 g. Due to lab error, the leaf litter
sample from tree 1 was not analyzed. For this set of samples, the mean leaf litter carbon percentage was
28.76% with a standard deviation of 3.33%, while the mean wood litter carbon percentage was 40.21%
with a standard deviation of 2.55%.

Table 9. Litter characteristics associated with 6 trees sampled at Southern Turf breadfruit orchard on Oahu island.						
Tree	DBH (cm)	Area m²	Leaf Mass (g)	Wood Mass (g)	%C Leaf	%C Wood
1	120	28.616	172.52	15.55		42.57
2	38.5	27.020	118.69	12.81	31.59	37.09
3	42	18.343	224.61	28.08	29.76	37.91
4	35	11.993	371.15	69.39	28.87	41.82
5	40.25	17.549	286.65	51.98	24.12	38.9
6	50	15.545	272.8	70.76	25.1	42.98

795

4.4.3. Estimating Carbon per Tree and Hectare

We can multiply the average leaf and wood litter mass by their respective average carbon concentration and scale to the average litter field dimensions to estimate the total carbon in the litter layer of an individual tree, which equates to 0.538 kgC/tree. This can be compared against the carbon stored in the biomass, which based on a 10-year orchard in the previous section is 90.2 kgC/tree, suggesting that the litter component equates to ~0.6% of the carbon stored in the biomass in this situation.

800

4.5. Discussion

Although explorations into litter were limited, this exercise supports previous assertions that the standing litter pool is a relatively insignificant component of carbon in breadfruit orchards. In the simple case we present, carbon represents only 0.6% of the biomass of in the trees. Furthermore, the variation associated with the little layer was substantial, creating a large degree of error associated with this small contribution to the total carbon. As these trees were in the same orchard and subject to similar climatological and management techniques the variability should have been low, or perhaps it is more accurate to say that these conditions should represent relatively low variability of the system. It is therefore likely that under less standardized conditions the variability of the litter layer will be even higher. Although a more extensive study should be done to better quantify the contributions of litter, it is suggested that the litter component of breadfruit be ignored under the current state of knowledge.

805

810

Since we only sampled trees of one age, and at one site, the correlations across time and space that were conducted for tree biomass are not possible. Future work could aim to connect the standing litter pool to the size (e.g. DBH) of the tree, and to the environment to better capture total dynamics of these pools. Future work could also incorporate decomposition kinetics and parse the fraction of carbon that returns to the atmosphere and the part that becomes incorporated into the soil carbon pool through the particulate fraction or through the work of nematodes and other insects.

815

5.2. Background

5.2.1. Hot Water Extractable Carbon

855 A full discussion of the models of the interactions of the soil microbial community with soil mineralogy in
soil carbon dynamics lies beyond the scope of this thesis. However, because of its strong correlation with
soil microbial biomass, HWEC has been recommended as a measure of short-term changes in soil
organic carbon, and representative of carbon that is readily available to microbes which can, in turn, form
860 mineral-associated carbon that is stable in soils for a longer timeframe. This characteristic of HWEC
makes it a sensitive early indicator of changes to SOC owing to the effects of *A. altilis* agriculture or other
land use changes (Ghani, Dexter, and Perrott 2003).

5.2.2. Equivalent Soil Mass

This study will employ the Equivalent Soil Mass (ESM) method to obtain the most accurate description of
soil carbon. In soils heavily impacted by agricultural land use and management practices, it is necessary
865 to appropriately account for the compaction effects on soil bulk density. Not taking compaction into
account can lead to biased estimates of soil carbon (Melone et al. 2021). In areas or situations where
there is reasonable reason to believe that changes in land management will impact soil compaction, the
ESM method can more accurately play a role in answering questions about changes to soil carbon owing
to the change in land management practice (Wendt and Hauser 2013).

870 5.3. Methods

5.3.1. Site Description

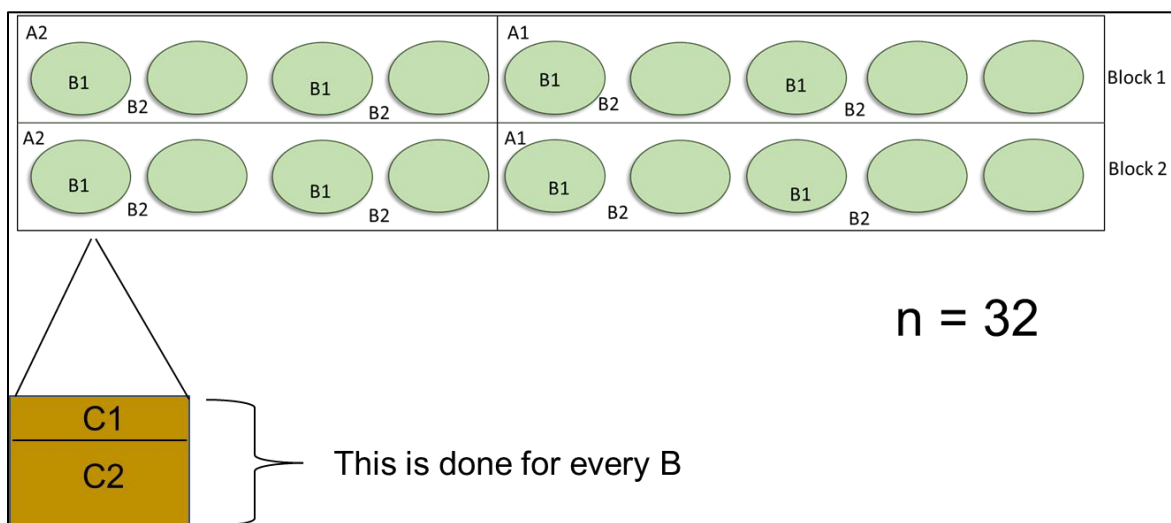
Sampling was conducted at Southern Turf in Mililani, Central O'ahu. The site has a long history of
intensive pineapple agriculture until the mid-1990s. Although much of this site is used as an active grass
turf farm, a portion of the site was dedicated to an *A. altilis* trial planting trial approximately nine years
875 ago. The site is dominated by highly weathered Oxisol soil. Oxisols are known for their low activity
mineralogy and their general lack of fertility (U.S. Department of Agriculture). According to the Climate
and Rainfall Atlas of Hawaii, the site receives 750-1350 mm of rainfall each year and a mean annual air
temperature of 20 – 22°C.

5.3.2. Sampling Description and Lab Work

880 Within an approximately 80m x 20m subsection⁶ of the orchard, we leveraged an existing planting density
trial to establish a split-plot design with two replicates (Figure 10). The main treatment is row-spacing:
wide (30ft) versus narrow (15ft) spacing of breadfruit trees. The split plot examines location: under the
breadfruit canopy and the open (grassed) areas between the plantings. At each sampling point, soils

⁶ Carbon accounting methodologies call for the sampling design to be based on terrain and site features. In the case of this relatively level field, no obvious features of the geography demanded a wider sampling area.

885 were sampled using a core of known volume by depth: shallow (0-30cm) and deep (30-60cm), or as deep as possible. This will result in a total sampling of 8 trees (4 in each spacing regime), 16 points (8 trees plus their corresponding between tree sampling), and 32 samples (16 shallow and 16 deep samples). This sampling design is depicted in the figure below. Samples were taken with a 2.54 cm diameter drill bit attached to a power drill and the soil was collected into a bucket with a hole in the bottom to effectively capture the drill spoil with minimal contamination from soil outside the sample site.



890

Figure 10. Schematic of the experimental design used to sample soils within an experimental breadfruit orchard that consists of two planting densities with wide (30 feet) and narrow (15 feet) spacing. The replicated block design sampled soils under the tree canopy and between the tree rows in both spacings, with soils sampled in a shallow (0-30cm) and deep (30-60cm) subsample.

895

Samples were immediately taken back to the lab for analysis. Total wet weight was recorded, and the samples were homogenized and subset. One subset was used to determine moisture content by obtaining the wet weight, and then determining the dry weight after soils were oven-dried at 60 °C for 48 hours. A second subset was sieved to 2mm, oven-dried at 60 °C, pulverized and encapsulated for total carbon analysis via an elemental analyzer. A third subset was sieved and used to conduct cold and hot water extractions to determine water-extractable carbon. Samples were first shaken in 20°C deionized water for 30 min, centrifuged, and the supernatant solution filtered through 0.45 µm membrane filters. Soils were then shaken in 80°C deionized water for 16 hours, and similarly treated as the cold-water extractable samples. The extracts were subsequently sampled for carbon concentration.

905

The design described above supports the statistical analysis of variation and comparison of means between main plots (wide vs. narrow) split plots (breadfruit vs. grass) by depth class. Treatment means and variance were compared using ANOVA, with statistical differences between groups determined with the Tukey means comparison. Because of the small sample size, this design will only detect relatively large differences focused within this area of the breadfruit orchard.

910 5.3.3. Equivalent Soil Mass (ESM)

To calculate the soil mass represented by a soil sample depth layer (DL) in terms of Mg ha⁻¹, we will divide the dry sample mass (recorded in grams) by the area sampled by the probe or auger, which is the cross-sectional area of its inside diameter and will calculate ESM as outlined in the equations below.

If D is expressed in mm, then the mass of the soil in Mg ha⁻¹ in each depth layer is calculated as:

915 Equation (14)
$$Soil_{Mass} = \frac{mass}{area} = \frac{Sample\ Mass}{(\pi \times \frac{D}{2})^2} \times 10000$$

The organic carbon (OC) mass in kg ha⁻¹ is the product of its soil mass and OC concentration.

Equation (15)
$$OC_{Mass} = Soil_{Mass} \times OC_{conc}$$

5.4. Results

5.4.1. Soil Mass

920 The soil was heavily compacted. Owing to the level of compaction, samples focused on two layers, shallow and deep, with the deep sample reaching just over 50cm. Based on the dry weight of the sample as calculated in the laboratory, the weight of each sample was converted from grams (g) to megagrams (Mg) and based on the probe diameter (2.54 cm), these results were converted to Mg per hectare.

The mean sample soil mass in Mg ha⁻¹ was found to be 2310.4 Mg/ha with a standard deviation of 639.9 Mg/ha. A significant difference between the shallow and deep layer samples was observed, with the shallow layer found to have an average of 2787.7 Mg/ha, while the deeper samples averaged 1832.95 Mg ha⁻¹.

5.4.2. Hot Water Extractable Carbon

930 There were no statistically significant differences found between interrow, canopy, wide or narrow soil samples at any depth. However, at both depths, there was consistently higher HWEC carbon found in the inter-row grassy area although the findings were not significant (Table 10).

Table 10. Results from the hot water extractable carbon on 32 samples collected from Southern Turf breadfruit orchard, demonstrating slightly higher levels occurring in the inter row areas compared to areas under the breadfruit canopy.		
	Inter row mg C/kg soil	Canopy mg C/kg soil
Shallow Layer	176.73	147.54
Deep Layer	94.15	86.69

935

5.4.3. Organic Carbon Heterogeneity

In general, the results of this work show carbon homogeneity in this Oxisol, suggesting that the relatively short history of *A. altalis* agroforestry on the site has not significantly shifted the carbon dynamics. Depth was the most significant source of carbon percentage heterogeneity across the site, with the shallower sampled layer containing statistically significant higher percent carbon and higher cold and hot water extractable carbon. Additionally, samples taken from the narrower planting had a statistically significant higher carbon percentage, but this did not translate into any significant differences between hot water extractable carbon between the narrow and wide planted row samples. No statistically significant differences in carbon percentage were found between samples taken from underneath the canopy or in the grassy/interrow area at any depth. Although not statistically significant, the samples taken from the inter-row grassy area consistently registered higher carbon. This held for percent carbon and cold and hot water extractable carbon. All results are displayed in Table 11.

Table 11. Results from hot water extractable and total soil carbon in 32 samples taken from Souther Turf breadfruit orchard on Oahu. Experimental design included comparing two planting densities (narrow and wide), the inter-row and beneath the canopy of breadfruit trees, and shallow (0-30cm) and deep (30-60cm) sampling.				
	Inter-row	Canopy	Narrow	Wide
Shallow % Carbon	1.97%	1.62%	1.92%	1.68%
Shallow Cold Water Extracted Carbon (mg/kg)	69.65	67.73	75.35	62.02
Shallow Hot Water Extracted Carbon (mg/kg)	176.73	147.54	171.20	153.07
Deep % Carbon	1.53%	1.34%	1.68%	1.19%
Deep Cold Water Extracted Carbon (mg/kg)	48.92	46.56	51.28	44.20
Deep Hot Water Extracted Carbon (mg/kg)	94.14	86.69	99.56	81.27

950

5.5 Discussion

As indicated in the introduction, the study design would only detect large differences in carbon quantity because of the relatively small sample size. Indeed, this study found a relatively homogenous soil carbon profile, and we could not conclude that breadfruit had a significant effect on soil carbon accumulation. However, this is a highly weathered Oxisol. Results may have been different in another soil that more readily forms soil organic carbon, such as an Andisol. The breadfruit orchard has not yet been in operation for a decade, and in this post-intensive agriculture, highly-weathered soil, carbon may simply accumulate more slowly.

955

960 HWEC is often an early indicator of changes to SOC. In this study, we found generally higher amounts of
HWEC in the grassy inter-row area. These findings are in line with literature that attributes greater SOC
accumulation to grasses as opposed to trees (Zhou et al. 2023; Wigley et al. 2020). The literature
generally notes that within tropical soils, tree cover has been found to not explain SOC concentration
(Zhou et al. 2023) and grasses have been found to trump trees in supporting soil carbon storage (Wigley
965 et al. 2020). However, the focus of this study was heterogeneity within the *A. altilis* agriculture area and
samples were not collected from nearby areas outside the *A. altilis* growing area; this study was not
designed to compare SOC accumulation associated with grasses versus trees, and therefore, additional
work is needed to more fully describe this relationship, and to better parse out the effects of breadfruit
trees on soil organic carbon versus the effects of crops or grasses grown in the rows between trees. If
970 properly elucidated, growing grasses or crops in the rows between trees is a potentially powerful way to
increase the total amount of carbon stored per hectare by leveraging the carbon storage strengths of both
trees (AGB) and grasses or other crops (soil organic carbon). Additionally, owing to the agricultural history
of this site, future work will need to account for plastic used in the management of pineapple – the carbon
figures noted above may unintentionally have incorporated plastic into the sample analyses.

975

980

985

6.1. Overview

As a long-lived tree crop, intuitively *A. altalis* has significant potential as a climate-smart, carbon credit-producing commodity. This study intended to apply a mix of carbon accounting methodologies and the scientific literature to develop quantitative data describing the terrestrial carbon pools of Hawaiian breadfruit orchards; specifically, the above-ground biomass (AGB) pool, the below-ground biomass (BGB) pool, the soil organic carbon pool and, the dead organic matter (litter) pool.

In the AGB pool, this study collected the data to: 1) develop growth equations based on environmental suitability, 2) to describe a relationship between stem diameter and carbon density, and 3) describe the relationship between terminal stem diameter and foliar mass and finally 4) to develop an allometric equation that describes total AGB. Using a published root-to-shoot ratio this robust AGB estimate also allowed us to estimate BGB. For this study, we also collected a suite of litter samples. Although the carbon methodologies tend to minimize the importance of this carbon pool, it is a part of the flow of carbon through the terrestrial landscape. Our findings here supported litter as quantitatively not a significant contributor of carbon storage. Finally, this study collected data on soil organic carbon, specifically looking for heterogeneity within the breadfruit orchard with an emphasis on hot water extractable carbon (HWEC). We found generally higher amounts of carbon in the grassy interrow area than under the breadfruit trees directly and although our sampling design did not allow for a comparison to soil samples outside the orchard, this finding potentially points to inter-cropping as a strategy to maximize carbon storage per hectare. Additionally, in another potentially important finding for carbon project design, the narrow planting held significantly higher %C.

We now have a foundational level of data from which we can begin to address a potential “climate-friendly” label for breadfruit. Much of this work lies beyond the scope of this current study, but included below is a rough outline of a way ahead to continue to build upon this work.

6.2. The Way Ahead: A Carbon Project

6.2.1. Carbon Accounting

The application of these findings may begin by employing the allometry developed here to develop a sampling plan for an active or planned breadfruit orchard, and the BGB, litter and soil methods could be used to complete the picture of total carbon. The Greenhouse Gas Protocol organization clearly delineates three scopes of emissions to consider when calculating an operation or product’s carbon footprint. A thorough carbon project would look at the emissions from both the perspective of a farmer, and the perspective of businesses and organizations that sell breadfruit and value-added versions of the project. In this approach, Tons of CO₂ stored per hectare is the starting point and Tons of CO₂ would be subtracted based on activities involved in breadfruit cultivation that produce CO₂. This could include

1025 applying fertilizer, driving vehicles to harvest, and driving vehicles to market, in addition to many other potential categories. In the case of value-added products, we would have to account for the CO₂ involved in packaging, cold storage, and production.

1030 Farmers are driven by a broad range of values that influence their decision-making process (Lincoln and Ardoin, 2015, 2016). While the economics of carbon markets may not be significant enough currently to drive a farmer to adopt breadfruit as a crop, other value-laden decisions, such as environmental or cultural values, may. Similarly, the market and associated economics of breadfruit are driven by consumption, with consumers equally driven by value-laden decisions (Lysak, Ritz and Henriksen 2019; Needham and Lincoln 2019). Therefore, while carbon markets may not be a substantial influence on farmer decisions at this time, it is possible to leverage other opportunities, such as consumer and farmer values to influence decision-making processes to promote the establishment of breadfruit production systems as a climate smart commodity.

6.2.2. *Calories per acre*

1040 Another important factor to consider is calories per acre; oftentimes when considering the carbon footprint of agricultural products, yields and effects to the food system are not incorporated into decision making. In the case of breadfruit, at conventional spacing, 50 trees are planted per acre. If each tree of the 50 trees produces 300 pounds or 136,078 grams of breadfruit and each gram has approximately 102 calories, then each acre of planted breadfruit produces 693,997,800 million calories while also containing a significant amount of carbon. By subtracting the CO₂ produced during breadfruit cultivation and during the value-added process, we'd be able to fit breadfruit into the literature which describes kg carbon emitted per 1000 calories.

1045 Alongside the research on human health associated with breadfruit consumption and the projected resilience of breadfruit in the face of climate change, the work of this thesis in describing the carbon content of breadfruit agroforestry provides a solid measure of breadfruit as a climate-smart commodity.

1050

1055

1060

7. REFERENCES

- Barančíková, G., Makovníková, J. and Halas, J.. 2016. "Effect of Land Use Change on Soil Organic Carbon." *Agriculture* 62 (1): 10–18. <https://doi.org/10.1515/agri-2016-0002>.
- Bauwens, S., Fayolle, A., Gourlet-Fleury, S., Ndjele, L.M., Mengal, C., and Lejeune, P.. 2017. "Terrestrial Photogrammetry: A Non-Destructive Method for Modelling Irregularly Shaped Tropical Tree Trunks." *Methods in Ecology and Evolution* 8 (4): 460–71.
- 1065 Berning, E. H., Andersen, C. V. H., Mertz, O., Dickinson, N., Opgenorth, M., Lincoln, N. K., ... & Rønsted, N. 2022. "Resilience of breadfruit agro-ecosystems in Hawai'i during the COVID-19 pandemic." *CABI Agriculture and Bioscience* 3 (1): 56.
- Brown, S. 1997. *Estimating Biomass and Biomass Change of Tropical Forests: A Primer*. Vol. 134. Food & Agriculture Org.
- 1070 ———. 2002. "Measuring Carbon in Forests: Current Status and Future Challenges." *Environmental Pollution* 116 (3): 363–72.
- Burdon, R. D., Kibblewhite, R.P., Walker, J.C.F., Megraw, R.A., Evans, R., and Cown, D.J.. 2004. "Juvenile versus Mature Wood: A New Concept, Orthogonal to Corewood versus Outerwood, with Special Reference to *Pinus radiata* and *P. taeda*." *Forest Science* 50 (4): 399–415.
- 1075 Chave, J., C. Andalo, S. Brown, M. A. Cairns, J. Q. Chambers, D. Eamus, H. Fölster, et al. 2005. "Tree Allometry and Improved Estimation of Carbon Stocks and Balance in Tropical Forests." *Ecologia* 145 (1): 87–99. <https://doi.org/10.1007/s00442-005-0100-x>.
- Cienciala, E., Russ, R., Šantr, H., Altman, J., Kopáček, J., Iva H, Štěpánek, P., Oulehle, F., Tumajer, J., and Stáhl, G.. 2016. "Discerning Environmental Factors Affecting Current Tree Growth in Central Europe." *Science of the Total Environment* 573: 541–54.
- 1080 Cotrufo, M.F., Wallenstein, M.D., Boot, C.M., Deneff, K., and Paul, E. 2013. "The Microbial Efficiency Matrix Stabilization (MEMS) Framework Integrates Plant Litter Decomposition with Soil Organic Matter Stabilization: Do Labile Plant Inputs Form Stable Soil Organic Matter?" *Global Change Biology* 19 (4): 988–95.
- 1085 Crow, S E., Deem, L.M., Sierra, C.A., and Wells, J.M.. 2018. "Belowground Carbon Dynamics in Tropical Perennial C4 Grass Agroecosystems." *Frontiers in Environmental Science* 6: 18.
- Cunia, T. 1965. "Some Theory on Reliability of Volume Estimates in a Forest Inventory Sample." *Forest Science* 11 (1): 115–28.
- 1090 Daba, D.E., and Soromessa, T. 2019. "The Accuracy of Species-Specific Allometric Equations for Estimating Aboveground Biomass in Tropical Moist Montane Forests: Case Study of *Albizia grandibracteata* and *Trichilia dregeana*." *Carbon Balance and Management* 14: 1–13.
- Das, T., and Das, A.K.. 2010. "Litter Production and Decomposition in the Forested Areas of Traditional Home Gardens: A Case Study from Barak Valley, Assam, Northeast India." *Agroforestry Systems* 79: 157–70.
- 1095 Dietze, M.C., Wolosin, M.S., and Clark, J.S.. 2008. "Capturing Diversity and Interspecific Variability in Allometries: A Hierarchical Approach." *Forest Ecology and Management* 256 (11): 1939–48.
- Erland, L. A., Needham, A. M., Kehinde, A. Z., Adebowale, A. P., Lincoln, N. K., Ragone, D., & Murch, S. J. 2023. "Impact of microclimate on *Artocarpus altilis* (Parkinson) Fosberg var *Ma'afala* fruit and nutritional quality." *Journal of Food Composition and Analysis*, 115, 104983.
- 1100 FAO. 2021. *Climate-Smart Agriculture Case Studies 2021*. Rome: FAO. <https://doi.org/10.4060/cb5359en>.
- Garnett, T. 2013. "Food sustainability: problems, perspectives and solutions." *Proceedings of the nutrition society*, 72 (1): 29-39.

- 1105 Ghani, A., Dexter, M., and Perrott, K.W. 2003. "Hot-Water Extractable Carbon in Soils: A Sensitive Measurement for Determining Impacts of Fertilization, Grazing and Cultivation." *Soil Biology and Biochemistry* 35 (9): 1231–43.
- Goodman, R.C., Phillips, O.L., and Baker, T.R. 2014. "The Importance of Crown Dimensions to Improve Tropical Tree Biomass Estimates." *Ecological Applications* 24 (4): 680–98.
- 1110 <https://doi.org/10.1890/13-0070.1>.
- Hann, D.W., and Larsen, D.R.. 1991. "Diameter Growth Equations for Fourteen Tree Species in Southwest Oregon." <https://ir.library.oregonstate.edu/dspace/handle/1957/7967>.
- IPCC. 2019. "2019 Refinement to the 2006 IPCC Guidelines for National Greenhouse Gas Inventories." In . <https://www.ipcc.ch/report/2019-refinement-to-the-2006-ipcc-guidelines-for-national-greenhouse-gas-inventories/>.
- 1115 Isaac, S.R., and Nair, M.A.. 2006. "Decomposition of Wild Jack (*Artocarpus Hirsutus*) Leaf Litter under Subcanopy and Open Conditions." *Journal of Tropical Agriculture* 42: 29–32.
- Jamaludheen, V., and Kumar, B.M. 1999. "Litter of Multipurpose Trees in Kerala, India: Variations in the Amount, Quality, Decay Rates and Release of Nutrients." *Forest Ecology and Management* 115
- 1120 (1): 1–11.
- Jones, A.M.P., Ragone, D., Aiona, K., Lane, W.A., and Murch, S.J. 2011. "Nutritional and Morphological Diversity of Breadfruit (*Artocarpus*, Moraceae): Identification of Elite Cultivars for Food Security." *Journal of Food Composition and Analysis* 24 (8): 1091–1102.
- Karpina, M., Jarzabek-Rychard, M., Tymków, P., and Borkowski, A. 2016. "UAV-Based Automatic Tree Growth Measurement for Biomass Estimation." *The International Archives of the Photogrammetry, Remote Sensing and Spatial Information Sciences* 41: 685–88.
- 1125 Ketterings, Q. M., Coe, R., van Noordwijk, M., and Palm, C.A. 2001. "Reducing Uncertainty in the Use of Allometric Biomass Equations for Predicting Above-Ground Tree Biomass in Mixed Secondary Forests." *Forest Ecology and Management* 146 (1–3): 199–209.
- 1130 Kora, S.A.H., Guendehou, G.H.S., Assogbadjo, A.E., Sinsin, B., and Goussanou, C.A.. 2019. "Allometric Equations from a Non-Destructive Approach for Biomass Prediction in Natural Forest and Plantation in West Africa." *Southern Forests: A Journal of Forest Science* 81 (2): 111–22.
- Langston, B.J. and Lincoln, N.K. 2018. "The role of breadfruit in biocultural restoration and sustainability in Hawai'i." *Sustainability* 10 (11): 3965.
- 1135 Lincoln, N. K. 2020a. "Agroforestry form and ecological adaptation in ancient Hawai'i: extent of the pākukui swidden system of Hāmākua, Hawai'i Island." *Agricultural Systems* 181: 102808.
- Lincoln, N.K. 2020b. "The State of our Starch." In Goodyear-Ka'ōpua, N., Howes, C., Osorio, J. K. K. O., & Yamashiro, A. [eds] *The Value of Hawai'i 3: Hulihia, the Turning*. University of Hawai'i Press; Honolulu, Hawai'i, USA.
- 1140 Lincoln, N., & Ladefoged, T. 2014. "Agroecology of pre-contact Hawaiian dryland farming: the spatial extent, yield and social impact of Hawaiian breadfruit groves in Kona, Hawai'i." *Journal of Archaeological Science* 49: 192-202.
- Lincoln, N, & Ardoin, N. 2016a. "Farmer Typologies: Who is Farming How and What." *Food, Culture, and Environment* 19 (3): 563-585.
- 1145 Lincoln, N., & Ardoin, N. 2016b. "Cultivating Values: Environmental Values and Sense of Place as Predictors for Sustainable Agricultural Practices in Five Categories." *Agriculture and Human Values* 33 (2): 389-401.
- Lincoln, N.K and Vitousek, P.M. 2017. Indigenous Polynesian Agriculture in Hawai'i. *Oxford Research Encyclopedias: Environmental Science* March (2017). DOI:
- 1150 [10.1093/acrefore/9780199389414.013.376](https://doi.org/10.1093/acrefore/9780199389414.013.376)

- Lincoln, N.K., Haensel, T.P., and Lee, T.M. 2023. "Modeling Hawaiian Agroecology: Depicting Traditional Adaptation to the World's Most Diverse Environment." *Frontiers in Sustainable Food Systems* 7: 1116929.
- 1155 Lincoln, N.K., Ragone, D., Zerega, N.J.C., Roberts-Nkrumah, L.B., Merlin, M., and Jones, A.M.P. 2018. "Grow Us Our Daily Bread: A Review of Breadfruit Cultivation in Traditional and Contemporary Systems." *Horticultural Reviews* 46: 299–384.
- Litton, C.M., and Kauffman, J.B.. 2008. "Allometric Models for Predicting Aboveground Biomass in Two Widespread Woody Plants in Hawaii." *Biotropica* 40 (3): 313–20.
<https://doi.org/10.1111/j.1744-7429.2007.00383.x>.
- 1160 Lucas, M.P., and Ragone, D. 2012. "Will Breadfruit Solve the World Hunger Crisis." *New Developments in an Innovative Food Crop. PIOJ Sustainable Development & Regional Planning Division* 5: 17.
- Lysák, M., Ritz, C., & Henriksen, C. B. 2019. "Assessing consumer acceptance and willingness to pay for novel value-added products made from breadfruit in the Hawaiian Islands." *Sustainability* 11 (11): 3135.
- 1165 Mausio, K, Miura, T. and Lincoln, N.K. 2020. "Cultivation Potential Projections of Breadfruit (*Artocarpus Altilis*) under Climate Change Scenarios Using an Empirically Validated Suitability Model Calibrated in Hawai'i." *Plos One* 15 (5): e0228552.
- Melone, A., Leah B.L., Crow, S.E., Hastings, Z., Winter, K.B., Ticktin, T., Rii, Y.M., Wong, M., Kukea-Shultz, K. and Watson, S.J. 2021. "Assessing Baseline Carbon Stocks for Forest Transitions: A Case Study of Agroforestry Restoration from Hawai'i." *Agriculture* 11 (3): 189.
- 1170 Mokany, K., Raison, R.J., and Prokushkin, A.S.. 2006. "Critical Analysis of Root : Shoot Ratios in Terrestrial Biomes." *Global Change Biology* 12 (1): 84–96. <https://doi.org/10.1111/j.1365-2486.2005.001043.x>.
- 1175 Needham, A., & Lincoln, N. 2019. "Interactions between People and Breadfruit in Hawai'i: Consumption, Preparation, and Sourcing Patterns." *Sustainability* 11 (18): 4983.
- Needham, A., Jha, R. and Lincoln, N.K. 2020. "The Response of Breadfruit Nutrition to Local Climate and Soil: A Review." *Journal of Food Composition and Analysis* 88: 103451.
- Padulosi, S., Hodgkin, T., Williams, J.T., and Haq, N. 2002. "Underutilized Crops: Trends, Challenges and Opportunities in the 21st Century." In *Managing Plant Genetic Diversity. Proceedings of an International Conference, Kuala Lumpur, Malaysia, 12-16 June 2000*, 323–38. CABI Publishing Wallingford UK. <https://www.cabidigitallibrary.org/doi/abs/10.1079/9780851995229.0323>.
- 1180 Paustian, K., Collier, S., Baldock, J., Burgess, R., Creque, J., DeLonge, M., Dungait, J., Ellert, B., Frank, S., and Goddard, T. 2019. "Quantifying Carbon for Agricultural Soil Management: From the Current Status toward a Global Soil Information System." *Carbon Management* 10 (6): 567–87.
- 1185 Picard, N., Rutishauser, E., Ploton, P., Ngomanda, A., and Henry, M. 2015. "Should Tree Biomass Allometry Be Restricted to Power Models?" *Forest Ecology and Management* 353: 156–63.
- Picard, N., Saint-Andre, L., and Henry, M. 2012. "Manual for Building Tree Volume and Biomass Allometric Equations: From Field Measurement to Prediction."
- 1190 Quintus, S., Huebert, J., Kirch, P. V., Lincoln, N. K., & Maxwell, J. 2019. "Qualities and contributions of agroforestry practices and novel forests in pre-European Polynesia and the Polynesian outliers." *Human Ecology* 47: 811-825.
- Rockström, J., Edenhofer, O., Gaertner, J., & DeClerck, F. 2020. "Planet-proofing the global food system." *Nature Food* 1 (1): 3-5.
- 1195 Santos Martin, F., R. M. Navarro-Cerrillo, R. Mulia, and M. Van Noordwijk. 2010. "Allometric Equations Based on a Fractal Branching Model for Estimating Aboveground Biomass of Four Native Tree Species in the Philippines." *Agroforestry Systems* 78 (3): 193–202.
<https://doi.org/10.1007/s10457-009-9271-5>.
- Stevens, C.F. 2009. "Darwin and Huxley Revisited: The Origin of Allometry." *Journal of Biology* 8 (2): 1–7.

- 1200 Tangjang, S., A. Arunachalam, K. Arunachalam, and S. Deb. 2015. "Litterfall, Decomposition and Nutrient Dynamics in Traditional Agro-Forestry Systems of Northeast India." *Ecology and Environmental Sciences, New Delh* 41 (1–2): 43–53.
- Wendt, J. W., and S. Hauser. 2013. "An Equivalent Soil Mass Procedure for Monitoring Soil Organic Carbon in Multiple Soil Layers." *European Journal of Soil Science* 64 (1): 58–65.
- 1205 West, G. B., Brown, J.H., and Enquist, B.J. 1997. "A General Model for the Origin of Allometric Scaling Laws in Biology." *Science* 276 (5309): 122–26. <https://doi.org/10.1126/science.276.5309.122>.
- Wigley, B.J., Augustine, D.J., Coetsee, C., Ratnam, J., and Sankaran, M. 2020. "Grasses Continue to Trump Trees at Soil Carbon Sequestration Following Herbivore Exclusion in a Semiarid African Savanna." *Ecology* 101 (5): e03008.
- 1210 Winter, K., Lincoln, N., Berkes, F., Alegado, R., Kurashima, N., Frank, K., ... & Toonen, R. 2020. "Ecomimicry in Indigenous resource management: optimizing ecosystem services to achieve resource abundance, with examples from Hawai'i." *Ecology and Society* 25(2).
- Yang, L., Zerega, N., Montgomery, A., and Horton, D.E. 2022. "Potential of Breadfruit Cultivation to Contribute to Climate-Resilient Low Latitude Food Systems." *PLoS Climate* 1 (8): e0000062.
- 1215 Yerton, S. 2019. "Air Travel's Carbon Footprint Takes A Big Environmental Toll In Hawaii." Honolulu Civil Beat. August 27, 2019. <https://www.civilbeat.org/2019/08/air-travels-carbon-footprint-takes-a-big-environmental-toll-in-hawaii/>.
- Zhou, X., Schoeneberger, M.M., Brandle, J.R., Awada, T.N., Chu, J., Martin, D.L., Li, J., Li, Y., and Mize, C.W.. 2015. "Analyzing the Uncertainties in Use of Forest-Derived Biomass Equations for Open-Grown Trees in Agricultural Land." *Forest Science* 61 (1): 144–61.
- 1220 Zhou, Y., Bomfim, B., Bond, W.J., Boutton, T.W., Case, M.F., Coetsee, C., Davies, A.B., ebruary, E.C., Gray, E.F., and Silva, L.C.R. 2023. "Soil Carbon in Tropical Savannas Mostly Derived from Grasses." *Nature Geoscience* 16 (8): 710–16.